

'The definitive version is available at www.blackwell-synergy.com'.

Late Pleistocene glacial and lake history of NW Russia

EILIV LARSEN, KURT H. KJÆR, IGOR N. DEMIDOV, SVEND FUNDER, KARI GRØSFJELD, MICHAEL HOUMARK-NIELSEN, MARIA JENSEN, HENRIETTE LINGE AND ASTRID LYSÅ

Larsen, E., Kjær, K.H., Demidov, I., Funder, S., Grøsfjeld, K., Houmark-Nielsen, M., Jensen, M., Linge, H. & Lyså, A.: Late Pleistocene glacial and lake history of NW Russia. *Boreas* Vol. Xx, pp. xx-xx.

Five regionally significant Weichselian glacial events, each separated by terrestrial and marine interstadial conditions are described from northwest Russia. The first glacial event took place in the Early Weichselian. An ice sheet centered in the Kara Sea area dammed up a large lake in the Pechora lowland. Water was discharged across a threshold on the Timan ridge and via an ice-free corridor between the Scandinavian Ice Sheet and the Kara Sea Ice Sheet to the west and north into the Barents Sea. The next glaciation occurred around 75-70 kyr BP after an interstadial episode that lasted *c.* 15 kyr. A local ice cap developed over the Timan ridge at the transition to the Middle Weichselian. Shortly after deglaciation of the Timan ice cap, an ice sheet centered in the Barents Sea reached the area. The configuration of this ice sheet suggests that it was confluent with the Scandinavian Ice Sheet. Consequently, around 70-65 kyr BP a huge ice dammed lake formed in the White Sea basin (the "White Sea Lake"), only now the outlet across the Timan ridge discharged water eastward into the Pechora area. The Barents Sea Ice Sheet likely suffered marine down-draw that led to its rapid

collapse. The White Sea Lake drained into the Barents Sea, and marine inundation and interstadial conditions followed between 65-55 kyr BP. The glaciation that followed was centred in the Kara Sea area around 55-45 kyr BP. Northward directed fluvial run off in the Arkhangelsk region indicates that the Kara Sea Ice Sheet was independent from the Scandinavian Ice Sheet and that the Barents Sea remained ice free. This glaciation was succeeded by a c. 20 kyr long ice-free and periglacial period before the Scandinavian Ice Sheet invaded from the west, and joined with the Barents Sea Ice Sheet in the northernmost areas of north-western Russia. The study area seems to be the only region that was invaded by all the three ice sheets during the Weichselian. A general increase in ice sheet size and the westwards migrating ice sheet dominance with time was reversed in Middle Weichselian time to an easterly dominated ice sheet configuration. This sequence of events resulted in a complex lake history with spill-ways being re-used and ice dammed lakes appearing at different places along the ice margins at different times.

Eiliv Larsen (e-mail: eiliv.larsen@ngu.no), Kari Grøsfjeld, Maria Jensen and Astrid Lyså, Geological Survey of Norway, N-7491 Trondheim, Norway; Kurt H. Kjær and Svend Funder, Geological Museum, University of Copenhagen, Øster Voldgade 5-7, DK-1350 Copenhagen K, Denmark; Igor N. Demidov, Russian Academy of Sciences, Karelian Research Centre, Institute of Geology, 11 Pushkinskaya Street, Petrozavodsk 185610, Russia; Michael Houmark-Nielsen, Geological Institute, University of Copenhagen, Øster Voldgade 10, DK-1350 Copenhagen K, Denmark; Henriette Linge, Bjerknes Centre for Climate Research, Allégaten 55, N-5007 Bergen, Norway.

Interpretation of the timing and dimensions of former shelf-based ice sheets invading mainland Russia has varied considerably. For the last glacial maximum about 20-18 kyr ago,

the reconstruction by Svendsen *et al.* (2004) is now generally accepted. This predicts a major reduction in ice sheet volume compared with Grosswald (1980, 1998), yet a considerable increase compared with the reconstructions of Velichko (1995) and Velichko *et al.* (1997). Numerical modelling of Eurasian ice sheet volumes through the entire Weichselian (Siegert *et al.* 2001; Lambeck *et al.* 2006) largely supports the recent reconstructions of Svendsen *et al.* (1999, 2004). These reconstructions invoke the blocking and rerouting of the large north-flowing Russian rivers, with the formation of large ice dammed lakes between the glaciers and the water divides to the south (e.g. Kvasov 1979; Arkhipov *et al.* 1995). Thus, the history of glaciers and lakes in mainland Russia are closely linked (e.g. Mangerud *et al.* 2001, 2004; Astakhov 2004; Svendsen *et al.* 2004). On the assumption that ice sheets from the Kara Sea, the Barents Sea and Scandinavia expanded simultaneously, it is predicted that about 90 kyr ago huge ice dammed lakes developed synchronously in western Siberia, the Pechora region and in the lowlands between the Gulf of Finland and the White Sea basin (Mangerud *et al.* 2001, 2004). However, there is still conflicting evidence regarding ice sheet and lake history in this region both in terms of timing, lake dimensions and drainage (e.g. Kjær *et al.* 2003; Mangerud *et al.* 2004; Svendsen *et al.* 2004).

The Arkhangelsk area, west of the Timan ridge, holds a key geographic position for studying glacier and lake history as ice sheets from the three centers, the Kara Sea, the Barents Sea and Scandinavia, terminated within the region during the Weichselian (Fig. 1). Topographically, the area is dominated by the wide, gently northward sloping river valleys. The two largest drainage basins, the Severnaya Dvina and Mezen, are separated by the Kuloi plateau, which reaches elevations of a little more than 200 m a.s.l. The south-north trending Timan ridge has a maximum elevation just above 300 m a.s.l., and separates the Mezen drainage basin from the Pechora basin to the east. In the north, the Timan ridge turns to the northwest across the Choshskaya Bay to form a bedrock ridge along the northern Kanin

Peninsula with maximum elevation close to 250 m a.s.l. In the lows the bedrock is buried, except for outcrops at the base of some of the sections. The glacial landforms are dominated by hummocky moraines and ice-marginal ridges, and with fluvial and lacustrine terraces. Three prominent end-moraine belts representing maximum positions of glacier advances exist (Fig. 1), the Syurzi Moraines between the upper reaches of the Pyoza and Mezen rivers (Chebotareva 1977; Lavrov 1991; Demidov *et al.* 2004), the Pyoza Moraines trending sub-parallel to the river Pyoza (Korchagin 1937; Krasnov *et al.* 1971; Lavrov 1975, 1977; Astakhov *et al.* 1999; Houmark-Nielsen *et al.* 2001), and the Scandinavian maximum moraines in the western part of the region (Larsen *et al.* 1999; Demidov *et al.* 2004; Demidov *et al.* 2006). End moraine belts representing deglacial stages occur to the west and north, respectively of the main ice marginal zones (Demidov *et al.* 2006; Kjær *et al.* 2006).

It is now evident that during the Late Weichselian the Scandinavian and the Barents Sea ice sheets merged north of the present study area, and that only Scandinavian ice reached the western parts of the area (Landvik *et al.* 1998; Larsen *et al.* 1999; Lyså *et al.* 2001; Demidov *et al.* 2006). In contrast, during the Early and Middle Weichselian, ice sheets from the Barents Sea and Kara Sea entered the Russian mainland, whereas ice originating in Scandinavia was absent (Svendsen *et al.* 2004). In recent literature the distinction between the Barents Sea and the Kara Sea Ice Sheets has been vague (Polyak *et al.* 2000; Mangerud *et al.* 2004; Svendsen *et al.* 2004). Kjær *et al.* (2006) shows, however, that there was a clear separation in time between Middle Weichselian Barents Sea and subsequent Kara Sea dominated ice sheets, implying a very dynamic glaciation history including large pro-glacial lakes that shift laterally through time. Currently, the glacial and lake history conflicts both within and between regions in NW Russia. In the Pechora region till deposits have yet to be correlated with glaciolacustrine sediments from the Early Weichselian Lake Komi, whilst no glaciolacustrine deposits have been identified for the large Middle Weichselian ice-dammed

lake in the White Sea area (Mangerud *et al.* 2001, 2004; Kjær *et al.* 2003, 2006). Between the Pechora and Arkhangelsk areas there are disagreements both regarding the number of Weichselian glaciations and corresponding lake correlations (Houmark-Nielsen *et al.* 2001; Kjær *et al.* 2003, 2006; Mangerud *et al.* 2004; Svendsen *et al.* 2004). The reconstruction of Svendsen *et al.* (2004) suggests that ice sheet activity was most pronounced in the Kara Sea during the Early Weichselian, shifting westwards to the Barents Sea and Scandinavia during the Middle and Late Weichselian. The more complex glaciation pattern introduced by Kjær *et al.* (2006) might be regarded as a second order cycle to the overall picture of Svendsen *et al.* (2004) characterised by distinct shifts between eastern and western dominated ice centres.

The main purpose of this paper is to present a synthesis of glacial and corresponding lake history of northwest Russia. We do so by first erecting a composite stratigraphy of the area independent of absolute chronology, thereafter discussing this stratigraphy before establishing absolute chronology. The Eemian to Late Weichselian environmental events are presented as a series of palaeogeographical reconstructions of the study area. As the new reconstructions presented herein implies a quite different glacial and lake history for the Early and Middle Weichselian than those published recently by Svendsen *et al.* (2004) and Mangerud *et al.* (2004), the implications at ice sheet scale are discussed both in terms of extent, dynamics and corresponding lakes.

Methodology

Ice marginal zones, originally mapped by Russian geological surveys, have been re-analysed using satellite imagery and air-photos. The principal methods in the field have been sedimentological, biostratigraphical, and structural geological investigations of deposits exposed in river and coastal sections. A variety of ice-flow directional elements like large-

scale glaciotectonics (Larsen *et al.* 2006), till fabrics, striations on clasts in tills and till provenance studies (e.g. Kjær *et al.* 2001) were applied. Further paleoenvironmental information is extracted from the sediments using pollen, molluscs, dinoflagellate cysts and foraminifera (Devyatova 1982; Houmark-Nielsen *et al.* 2001; Funder *et al.* 2002; Grøsfjeld *et al.* 2006; Larsen *et al.* 2006).

Sections were sketched in the field, and logged using vertical resolution between 1:10 and 1:100. Sorted sediments were classified following Eyles *et al.* (1983), whereas diamict sediments were described and classified according to Krüger & Kjær (1999).

Informal, geographical names are used for regionally important till units (Larsen *et al.* 1999; Houmark-Nielsen *et al.* 2001; Kjær *et al.* 2003, 2006; cf. Fig. 2). The term Mezen Interstadial is used for a Middle Weichselian ice-free period with raised marine sediments first recorded in the Mezen Bay area (Kjær *et al.* 2003; Jensen *et al.* 2006).

All Optically Stimulated Luminescence (OSL) dates were obtained from the Nordic Laboratory for Luminescence Dating, Risø, Denmark. The single aliquot regenerative dose protocol applied to quartz grains was used to estimate the equivalent dose (Murray & Wintle 2000). The samples were analyzed for natural series radionuclide concentrations in the laboratory, using high-resolution gamma spectrometry (Murray *et al.* 1987). These concentrations were converted into dose rates using the conversion factors listed by Olley *et al.* (1996). Recently OSL ages have been corrected for sample burial depth as cosmogenic radiation decreases with increasing overburden (Mangerud *et al.* 2004; Thomas *et al.* 2006), this instead of assuming a constant burial depth of *c.* 4 m. However, as almost all published OSL results from Arkhangelsk and adjacent areas have not been converted into depth-specific ages, we have for the sake of compatibility only presented uncorrected ages (Table 1). Besides, the correction only in rare occasions moves the age estimate outside of one standard deviation of the uncorrected age and the mean change is small compared to the typical overall

age uncertainty of ~10% (Demidov *et al.* 2006; Kjær *et al.* 2006). The age estimates are plotted in Fig. 6 and listed in Table 1.

Conventional radiocarbon ages were made on terrestrial plants at the Trondheim dating laboratory. AMS radiocarbon dates were obtained from the Aarhus laboratory. Twigs were determined to species level before measurement. Calendar age estimates were obtained by using the program *Oxcal 3.10* with *IntCal* (Bronk 1995, 2001; Reimer *et al.* 2004). Age estimates are plotted in Fig. 6 and listed in Table 2.

Rock samples for *in situ* cosmogenic ^{10}Be surface exposure dating were collected in order to test the palaeogeographic reconstruction. BeO targets were processed at Washington State University, Vancouver, following the procedures described by Linge *et al.* (2006a). The ^{10}Be concentration was measured at the Tandem AMS facility at Gif-sur-Yvette (Raisbeck *et al.* 1994) relative to the NIST standard SRM 4325. Concentrations were corrected for procedural blanks, sample thickness and topographic shielding, and ages were calculated using a sea-level, high-latitude ^{10}Be production rate of 5.1 atoms per gram quartz per year (Stone 2000), as described in Linge *et al.* (2006a). No correction has been made for past changes in geomagnetic field intensity, presumably low above 40°N (Masarik *et al.* 2001). Age estimates are listed in Table 3 and plotted in Fig. 7.

Rationale behind the stratigraphic model

By using marine beds in strategic positions as stratigraphic markers and due to the generally good stratigraphic record, it was possible to construct a composite stratigraphic model independent of absolute chronology for the Arkhangelsk region (Fig. 2). This allows us to first develop the stratigraphy then test this by applying absolute dating techniques.

Marine marker beds

Eemian marine sediments are widespread along the Severnaya Dvina, Pyoza and Mezen rivers, and on the Kanin Peninsula. This was summarised by Biske & Devyatova (1965) and Devyatova (1982), and more recently by Houmark-Nielsen *et al.* (2001), Lyså *et al.* (2001), Funder *et al.* (2002), Nielsen & Funder (2003) and Grøsfjeld *et al.* (2006). The Eemian sediments from northern Russia are traditionally distinguished by their “warm” boreal components in the mollusc fauna, *i.e.* species that presently have their northern limit on the Norwegian or Murman coasts. From their oceanic temperature signal de Geer (1896) correlated these faunas with the Eemian marine faunas at the type-site in Holland. This was later confirmed by pollen analyses (Devyatova 1982; Funder *et al.* 2002). Older marine sediments with similar faunas (The Likhvin or Northern Transgression) have been described from localities at the upper Pyoza River (Biske & Devyatova 1965). However, as shown by Houmark-Nielsen *et al.* (2001) and Nielsen & Funder (2003) both the stratigraphical setting and OSL dates indicate that these occurrences belong to the Eemian. The much older (Pliocene or Early Pleistocene) Kolva and Padimei marine sediments are known from borings in the neighbouring Pechora Basin. These sediments show a development from deep to shallow water, ending with shoreface sediments with the extinct *Cyrtodaria angusta*. The sequence reflects a transition from arctic to boreal with several boreal indicators common with the Eemian (Merklin *et al.* 1979; Zharkidze 1983). Although our study has revealed a mollusc fauna with *Cyrtodaria angusta* at one locality, the heavily glacier-tectonised coastal cliff at northern Kanin Peninsula (Larsen *et al.* 2006), the stratigraphical setting of the marine Eemian sediments preclude confusion with these much older and deeper marine sediments. We therefore conclude with Zharkidze & Samoilovich (1989) that faunas similar to the Eemian are not known from any other mid to late Quaternary sites in northern Russia, and thus that the Eemian sediments form an important marker in the local stratigraphy.

The younger marine tidal sediments ascribed to the Mezen Interstadial were first identified in the Mezen Bay area (Kjær *et al.* 2003), and have since been observed both further west on the Kuloi coast and in the Choshskaya Bay area (Jensen *et al.* 2006). At Cape Tolstik the till at the base of the section contains abundant reworked boreal molluscs suggesting a post-Eemian age for the entire succession and accordingly also for Mezen Interstadial (Kjær *et al.* 2003; Nielsen & Funder 2003). A similar stratigraphic position for the interstadial has since then been demonstrated for a number of sites (Jensen *et al.* 2006). This unit is stratigraphically above a till of the Barents Sea Ice Sheet and below a till of the Kara Sea Ice Sheet making it very useful for reconstructing sequences of glacial events (Kjær *et al.* 2006).

Developing the composite stratigraphic model (Fig. 2)

In the stratigraphic scheme of the Arkhangelsk region (Fig. 2), we have chosen to define stratigraphic positions (SP 1-11) rather than using units, as several different sedimentary environments are present at each stratigraphic level.

The Cape Tolstik site (Site 4, Fig. 1, Fig. 3D) is a key for erecting the regional stratigraphy as three of the five regional tills with intervening sediments occur in superposition along a more than 4 km long coastal cliff (Ramsay 1904; Kjær *et al.* 2003). The lowermost unit at Cape Tolstik, the Yolkino Till, contains abundant boreal molluscs, and a post-Eemian age was assigned to it (Kjær *et al.* 2003). Between the Yolkino and Cape Tolstik tills there are deglacial and ice-proximal sediments, but no sediments representing full interstadial conditions. Between the Cape Tolstik and Syomzha tills there are shallow marine sediments from a sea level with maximum elevation some 40 metres above present (Kjær *et al.* 2003; Jensen *et al.* 2006). The succession at Cape Tolstik thus defines four stratigraphic positions (Fig. 2, SP 5-8).

From Cape Kargovsky, to the northwest of Cape Tolstik, stratigraphic positions 5, 7 and 8 can be event stratigraphically correlated with the Cape Tolstik site (Kjær *et al.* 2003). In addition, the Cape Kargovsky section is capped by a the Bobrovo Till (SP 10), containing abundant Scandinavian/Karelian crystalline pebbles clearly showing that it was deposited by the Scandinavian Ice Sheet (Kjær *et al.* 2003; Demidov *et al.* 2006). Only one till of Scandinavian origin is found in the area (Larsen *et al.* 1999; Demidov *et al.* 2006), this being stratigraphically younger than the Syomzha Till (SP 8). Fluvial sediments below the Bobrovo Till along Severnaya Dvina overlaps in time with marine and glacial conditions in the Mezen Bay are due to regional differences in glaciation history (Fig. 2, SP 7-9).

At Pestsovaya (Site 7, Fig. 1), a till deposited by ice moving from the NE occurs stratigraphically above Eemian marine sediments (Kjær *et al.* 2006). This till lies below the Cape Tolstik Till, and based on this site alone it might have any stratigraphic position between the Eemian and the Cape Tolstik Till, except the Yolokino Till which would be expected to indicate ice movement from the SE. In the upper parts of river Pyoza ice-proximal sediments of post Eemian age are separated from the above lying Yolokino Till (SP 5) by fluvial and lacustrine sediments that indicate full interstadial conditions (Houmark-Nielsen *et al.* 2001). These ice-proximal sediments must relate to a pre SP 5 glaciation followed by ice-free conditions (SP 3-4). Thus an SP 2 glaciation from the NE is evident from these sites.

Eemian to Late Weichselian stratigraphy

Based on the rationale behind constructing the composite stratigraphic model as outlined above (Fig. 2), the sediments occupying the different stratigraphic positions can be described collectively. Five profiles showing the regional stratigraphy are plotted on the map (Fig. 1) and shown as Fig. 3.

SP 1: Eemian marine

Marine Eemian sediments are found along most river valleys (Devyatova 1982; Houmark-Nielsen *et al.* 2001; Lyså *et al.* 2001; Funder *et al.* 2002; Nielsen & Funder 2003; Grøsfjeld *et al.* 2006; Lambeck *et al.* 2006), and are less frequent along the coasts of the area. Along the river Severnaya Dvina, above 35 m a.s.l., lagoonal marine sediments underlie peat of Early-Mid Eemian age, deposited after regression (Devyatova 1982; Lavrushin & Spiridonova 1995). The marine sediments range from a spatially restricted Late Saalian glaciomarine diamicton deposited during deglacial flooding, to offshore and shoreface sediments deposited during the succeeding regressive phase (Figs 4A, 6A; Lyså *et al.* 2001; Nielsen & Funder 2003; Grøsfjeld *et al.* 2006). The glaciomarine diamicton is characterised by sparse arctic faunas, but warmer than present boreal mollusc species that entered the area immediately after the beginning of the Eemian (Funder *et al.* 2002; Grøsfjeld *et al.* 2006; Lambeck *et al.* 2006). Owing to isostatic emergence and regression the late Eemian only occurs in few exposures (Grøsfjeld *et al.* 2006)

SP 2: Fluvial, lacustrine and shallow marine

The sediments attributed to this position occur on the north coast of the Kanin Peninsula (Fig. 4B) upthrust by glaciers moving from the north (Larsen *et al.* 2006). It is suggested that these sediments were deposited in the earliest part of the Weichselian at a sea-level slightly below present (Larsen *et al.* 2006). The lower part consists of lacustrine and fluvial sediments, whereas the upper is composed of tidal sediments. The succession is suggestive of shallow lake basins that were opened to the sea by coastal erosion (Larsen *et al.* 2006). The coastline at the time was located to the north of the present, and ran sub-parallel to it.

SP 3: Pestsovaya Till

Along the western shores of the Kanin Peninsula there are large sediment thicknesses (Figs 3D, 4C). At Pestsovaya and Tarkhanov a till deposited from the NE is found at the base of sections, and is followed upwards by a thick series mainly of sand and gravel (Fig. 4D; Kjær *et al.* 2006). This succession has been interpreted as a glacial-deglacial sequence with the sediments above the till being deposited during down-wasting of the ice as glacio-fluvial and proglacial deposits (Kjær *et al.* 2006). The sediments are tentatively event-correlated with ice-proximal sediments on the upper Pyoza described by Houmark-Nielsen *et al.* (2001). Further downstream on Pyoza these ice-marginal sediments pass into bedded sand and gravel with syngenetic ice-wedge casts, and show north and northwest paleocurrent directions. The latter sediments were deposited by a braided river system distally to the ice margin and with drainage directions as today (Houmark-Nielsen *et al.* 2001).

SP 4: Fluvial and lacustrine

Along the upper Pyoza, the ice marginal sediments (SP-3) pass upwards into bedded sand, mud and gyttja capped by more sandy sediments with increasing periglacial deformation structures towards the top. Pollen analyses carried out at two sites reveal a change from vegetation dominated by *Picea*, *Pinus sylvestris*, *Betula alba* and *B. nana* to an open herbaceous vegetation (Houmark-Nielsen *et al.* 2001). The mud and gyttja accumulated in small lakes, whereas the sandy sediments originated from braided rivers and eolian dunes (Houmark-Nielsen *et al.* 2001). Thus, after the first Weichselian glaciation (SP-3), full interstadial conditions developed.

SP 5: Yolkino Till

The Yolkino Till (Houmark-Nielsen *et al.* 2001; Kjær *et al.* 2001, 2003) is the lowermost unit at Cape Tolstik (Figs 3E and 5A). It is underlain by glaciofluvial sediments at many sites, and

along the upper Pyoza it grades upwards into glaciolacustrine sediments (Fig. 5B). The till is found along the river Pyoza and in the Mezen Bay area and shows consistent ice-movements from the east to east-southeast (Houmark-Nielsen *et al.* 2001; Kjær *et al.* 2003). This is the only till unit showing this directional pattern, and the regional distribution is compatible with ice centred east of the upper reaches of river Pyoza (Houmark-Nielsen *et al.* 2001; Kjær *et al.* 2003).

SP 6: Cape Tolstik Till

This till was deposited by ice moving from northern to northwestern directions and is found below tidal sediments in the Mezen Bay and Choshskaya Bay areas (Figs 3C, 3E and 5A; Kjær *et al.* 2003, 2006; Jensen *et al.* 2006). A till with this depositional direction also occurs along western Kanin Peninsula, as thrust sheets along northern Kanin (Kjær *et al.* 2006; Larsen *et al.* 2006), and as the youngest till bed along river Pyoza (Houmark-Nielsen *et al.* 2001). Thus, most of SP 6 is interpreted as a basal till deposited beneath a glacier that advanced from a north to north-westerly direction, but the lower part at Pyoza might have been deposited by melt-water in front of the advancing glacier. This might also account for the thickness in this area of 10 metres (Houmark-Nielsen *et al.* 2001).

SP 7: Mezen Interstadial, marine

The sediments representing this stratigraphic level are found *in situ*, up to 13.5 m above present high tide level in the Mezen Bay and upthrust in Choshskaya Bay to *c.* 30 metres (Kjær *et al.* 2003, 2006; Jensen *et al.* 2006). Most notable are beds of rhythmically laminated heterolithic deposits alternating with fine sand with current and wave generated ripples (Figs 5C, 5D). Within the heterolithic beds there are systematic changes in laminae thickness, and the laminae are arranged in couplets, single or double, typical for deposition in a tidal environment (Nio & Yang 1991). This facies association has been interpreted as deposited in

the sub-tidal zone (Jensen *et al.* 2006) at or just above storm wave base (Hampson & Storms 2003). Channel facies indicates shallower water depths, and sub- or inter-tidal formation. Cryoturbation at Syomzha indicates further shallowing and ultimately sub-areal exposure (Kjær *et al.* 2003).

SP 8: Syomzha Till

This till, showing an ice-flow direction from the NE, is found above the tidal sediments at Syomzha, Tolstik, Abramovsky and Oiva (Figs 3E, 5E). At Kargovsky (Fig. 3E), muddy and diamict sediments are found in the same stratigraphic position (Kjær *et al.* 2003). At Bolshoi Vzyglavnyie and Cape Zhelesnyie (Fig. 3C) the tidal sediments are glaciotectonically thrust from the NE (Fig. 5C), but the corresponding till bed is not found (Kjær *et al.* 2006). Glaciotectonic thrusting from the NE, younger than a thrusting event from the NW, is also evident from the northern Kanin coast (Larsen *et al.* 2006). The diamicton at Cape Kargovsky reaches up to 22 metres in thickness and is interpreted as ice marginal (Kjær *et al.* 2003). This may also be the case for part of the succession at Cape Abramovsky where thickness is up to 10 metres.

SP 9: Fluvial

This stratigraphic level comprises fluvial facies below the Bobrovo Till. The most complete succession is found in sections along the river Severnaya Dvina (Larsen *et al.* 1999; Lyså *et al.* 2001). The sediments have a lower erosive boundary (Fig. 5F), and show a development from shallow channel deposits with redeposited marine sediments, peat formation and followed by an upwards change into fluvial sediments with syngenetically developed ice wedges. Pollen analysis from a peat horizon shows taiga vegetation (Devyatova 1982).

SP 10: Bobrovo Till

This till containing crystalline pebbles of Scandinavian origin is widespread along the Severnaya Dvina and Vaga rivers north of an end moraine belt that represents the maximum extent of the Scandinavian Ice Sheet (Larsen *et al.* 1999; Lyså *et al.* 2001; Demidov *et al.* 2004; Demidov *et al.* 2006). South of this limit (Fig. 5G), glaciolacustrine sediments and fluvial/glaciofluvial sediments with drainage directions opposite to the present day are associated with this event. A till containing crystalline pebbles is also found at Cape Kargovsky (Kjær *et al.* 2003), at Koida, and at the Morzhovets Island. At Madakha and Oiva on the north coast of the Kanin Peninsula, till deposited from the NW and overlying glaciolacustrine sediments that are stratigraphically younger than SP 8 can also be attributed to the Bobrovo Till (Kjær *et al.* 2006). The glaciolacustrine sediments below the till (Fig. 5H) accumulated in proglacially lakes dammed by the advancing ice. Within the glaciolacustrine sediments three phases of sediment filling intervened by drainage of the basin are recognized (Jensen *et al.* 2005). This indicates that the ice margin was fluctuating somewhere north of the present coastline before reaching its maximum position.

SP 11: Late glacial

Two end moraine zones associated with retreat of Scandinavian ice are mapped in the western parts of the area. Between these zones, sections show evidence of melting of stagnant ice, and re-establishment of present river drainage regime (Larsen *et al.* 1999; Lyså *et al.* 2001; Demidov *et al.* 2006).

Chronology

The stratigraphy detailed above identifies five glacial events represented by five tills of post-Eemian age, interbedded with marine, fluvial or lacustrine sediments (Figs 2, 3). The

successions are dated by Optically Stimulated Luminescence (OSL) and radiocarbon techniques (Tables 1, 2). These results are complemented by cosmogenic dates from bedrock and erratic boulders across the study area (Table 3, Fig. 8; Linge *et al.* 2006b). Fig. 6 shows five compilations of dates designed to infer the depositional age of regional till units i.e. Pestsovaya Till (SP 3), Yolokino Till (SP 5), Cape Tolstik Till (SP 6), Syomzha Till (SP 8) and Bobrovo Till (SP 10). Only dates from sediment successions with a specific till unit or its depositional correlative are used to constrain its age. This also implies that dates from successions with multiple till units might appear in several compilations. For instance, dates derived from the Mezen Interstadial are used to infer ages of both the Cape Tolstik and Syomzha tills, respectively above and below the two till units. In the case of Pestsovaya Till (SP 3), Yolokino Till (SP 5) and Bobrovo Till (SP 10) dates of proglacial or deglacial sediments are weighted higher when inferring depositional age as these represent near time-equivalent sedimentation. Contrary, ages obtained from sediment below and above might deviate significantly from the actual age of ice advance over the area. It is noted though, regarding the Cape Tolstik Till (SP 6) and Syomzha Till (SP 8) that dates below and above allow only narrow time interval to be inferred for their deposition.

We adopt the chronology of Lambeck *et al.* (2006) by assigning an age of 130.5 kyr for the Saalian/Eemian boundary, and 119.5 kyr for the Eemian/Weichselian boundary. Three dates from marine sediments (Fig. 6A, SP 1), biostratigraphically correlated with the Eemian (Grøsfjeld *et al.* 2006), give ages that appear too young. The age of the overlying interstadial sediments (Fig. 2, SP 2) cannot be constrained directly by dates. Larsen *et al.* (2006), argue that these were deposited before the first Weichselian ice advance (SP 3). According to this and the age proposed below for SP 3, the interstadial (SP 2) occurred between 119.5 and 100 kyr BP.

The Pestsovaya Till (SP 3) is associated with proglacial and deglaciation sediments, the latter formed in lakes developing as the glacier stagnated and wasted away (Kjær *et al.* 2006). The majority of the dates from proglacial sediments are between 100-90 kyr, whereas the dates from the deglaciation sediments are all younger but have a large spread (Fig. 6A). The latter is not unexpected since these dates are from sediments deposited in lakes developing during and after deglaciation. Whether this represents the true duration is not known (Kjær *et al.* 2006). In accordance with most dates from proglacial sediments it is suggested that the age of SP 3 is about 100-90 kyr.

The minimum age of the Yolkino Till (SP 5) is constrained by a suite of dates that indicate deglaciation *c.* 70 kyr BP (Fig. 6B, SP 6-11). Three of the samples from proglacial sediments support deglaciation close to 60 kyr, whereas the other three are much older (SP 5-Upper). There is an overlap between samples from positions below the Yolkino Till and above it (SP 1-4 and SP 6-11), and the maximum age of the glaciation is only tentatively suggested to be 75 kyr. According to this chronology, the SP 4 interstadial lasted between 90 and 75 kyr BP.

The deglaciation after deposition of the Cape Tolstik Till (SP 6) is dated by samples from the overlying marine sand to about 65 kyr (Jensen *et al.* 2006; Fig. 6C, SP 7). There is some overlap between maximum dates of SP 6 (Fig. 6C, SP 1-6) and minimum dates of SP 5 (7B, SP 1-4). The field evidence shows deglaciation after deposition of the Yolkino Till (SP 5), but there is no indication of development of full interstadial conditions (Houmark-Nielsen *et al.* 2001; Kjær *et al.* 2003). The lower boundary of SP 6 is thus placed at 70 kyr BP in accordance with the age assignment of the upper boundary of SP 5. It is, however, realized that this leaves a short time span (75-65 kyr) for the sequence of SP 5-6 events (glaciation – deglaciation – glaciation – deglaciation). The old dates in the group SP 9-11 are from sediments deposited in a glaciolacustrine basin on northern Kanin Peninsula (Jensen *et al.*

2005). This is interpreted to have occurred during the advance that deposited the Bobrovo Till (SP 10). Clearly these dates are too old for the interpretation favoured in the present paper, but we argue that they do not represent depositional age. Firstly, the obtained ages are mostly pre-Eemian, but Eemian molluscs are frequent in sediments stratigraphically below the glaciolacustrine unit. Furthermore, if the age estimates were taken at face value, the consequence in terms of glacial history would be that the Weichselian as derived from other localities would mimic the pre-Eemian (Saalian) as would then be derived from northern Kanin Peninsula. Also, we suggest that the age spread alone is wider than expected for the duration of the glaciolacustrine sedimentation. Thus, it is believed that the sedimentary environment was turbid and that this caused insufficient zeroing of the material.

The dates from marine sand (Fig. 6D, SP 7) give both the duration of SP 7 (65-55 kyr BP) and the lower boundary of the Syomzha Till (SP 8) at 55 kyr BP. This maximum age is also well supported by the ages obtained from SP 1-6. The old ages in the group SP 9-11 are the same as those discarded in the discussion above. The upper boundary of SP 8 is poorly constrained as few dates cover the time window 50 to 20 kyr BP, but an age of 45 kyr is tentatively suggested. The Bobrovo Till is well dated to *c.* 20-17 ka BP both by underlying and proglacial sediments, and by radiocarbon dates from the deglaciation period (Fig. 6E). According to this chronology there was a long, ice-free period from about 45 to 20 kyr ago.

Fig. 7 shows the reconstructed ice margins with age assignments based on the developed OSL chronology. The cosmogenic dates are from bedrock and erratic boulders and are discussed in detail by Linge *et al.* this (2006b). Compared with the OSL chronology, many of the dates of bedrock from the Timan ridge are too young. This is explained by weathering of the non-resistant sandstones in the area (Linge *et al.* 2006b). According to this reconstruction, the two southernmost sites (sites 0206 and 0207, Fig. 7) on the Timan ridge were inside the area covered by the Timan glaciation. Taking the dates of erratics from these

two sites at face value, one might suggest that the Timan glaciation had the terminal position between the two sites, and that the northernmost site was ice-free since the Eemian. The erratics from the northernmost site on Timan (site 0208), and most dates from Kanin generally indicate deglaciation around 40-50 kyr BP, in agreement with the OSL chronology. One date from Kanin, the westernmost sample at the lowest altitude, gave an age of *c.* 18 kyr BP, supporting that this site was just within the ice-margin at the last glacial maximum.

Palaeogeographical changes: implications for Eurasian ice sheets and lakes

The main Eemian – Late Weichselian environmental changes recorded in the Arkhangelsk region of NW Russia are depicted in an event-stratigraphical model and a series palaeogeographical maps (Figs 8, 9). The recorded glacial history of the area has, according to our results significant consequences both for understanding interaction between the ice sheets and for their large-scale configuration (cf. Fig. 10).

The Eemian and the transition to the Weichselian

The Eemian marine sediments recorded in the area (Fig. 8) represent a large variety of shallow marine environments, and together span most of the 11 000 years of this interglacial. For 1500-2000 years in the early Eemian (Fig. 9A), there was a sea-passage between the White Sea and the Gulf of Bothnia (Funder *et al.* 2002). In the north, sea level after the Saalian deglaciation may have been more than 200 m above the present, while the southern parts, where isostasy was weaker, had maximum sea level of 50-100 m in the Early Eemian (Lambeck *et al.* 2006). Thus, in the Early Eemian the present river valleys were occupied by a shallow sea, and with a coastline up to 350 kilometres inland of the present (Fig. 9A). The reconstruction implies that river flow was northwards as today. Pollen analyses show that

taiga vegetation persisted all the way to the coast, and that mixed oak forest was closer than today (Devyatova 1982; Funder *et al.* 2002). Shallowing in the late Eemian resulted in diversification of local marine environments and a decrease in faunal richness.

There is a gap to the fluvial and shallow-marine sediments on northern Kanin Peninsula that represents a low sea-level stand in the early Weichselian (Figs 8, 11; Larsen *et al.* 2006). The northern Kanin Peninsula coastline at this time was parallel to and situated north of the present.

Kara Sea-dominated glaciation and Lake Komi, ca. 100-90 ka, and the following interstadial

Around 100-90 kyr BP a Kara Sea-dominated glaciation (SP-3) is recorded in the upper Pyoza area by ice proximal sediments (Fig. 8; Houmark-Nielsen *et al.* 2001). Down-valley these continue as fluvial sediments with western to northwestern drainage directions towards the Barents Sea. A till bed (Pestsovaya) deposited from the northeast and associated with a thick ice-marginal complex of this age on the western Kanin Peninsula (Kjær *et al.* 2006) suggests an ice margin as outlined in Fig. 9B. Nowhere outside of this ice-marginal position is a till unit with northeastern provenance found in this stratigraphic position. Thus, the data from the area suggest that the rivers were northbound and not blocked by ice in the north.

At this time glacier extent was at the Weichselian maximum in Russia according to Svendsen *et al.* (2004). The ice sheet penetrated far into Siberia (Fig. 10A). The westward extension along the Pechora lowland was considered unclear as no till can be identified from the area belonging to this event (Svendsen *et al.* 2004). In the Pechora lowlands the ice dammed a large lake, the Lake Komi, up to the elevation of the Tsilma pass in the Timan ridge, and Mangerud *et al.* (2004) concluded that Lake Komi was linked via this pass-point with a much larger lake in the White Sea basin. This implies ice damming north of the White Sea, and therefore these authors concluded that the Barents Sea Ice Sheet was confluent with

the Scandinavian Ice Sheet. However, this model is at odds with the data from the White Sea area described above (Fig. 9B), and our reconstruction suggests that the ice sheets were separate during this glaciation (Fig. 10A). This reconstruction does not question the existence of the Lake Komi, but does suggest that the Komi outlet was across the Tsilma pass-point in the Timan ridge and further towards the Barents Sea via the Mezen Bay area (Fig. 9B), and not from a White Sea lake towards the Baltic Sea as suggested by Maslenikova & Mangerud (2001) and Mangerud *et al.* (2004).

Following deglaciation, rivers continued to flow to the north as recorded in the Arkhangelsk region, whilst periglacial conditions prevailed (Figs 8, 9C). Pollen analyses from lake sediments shows both an open forest rich in shrubs and dominated by birch, pine and spruce, and a grass-rich steppe-tundra (Houmark-Nielsen *et al.* 2001). Along the river Severnaya Dvina, there is an erosional boundary between fluvial and underlying marine Eemian sediments (Fig. 8; Lyså *et al.* 2001). This erosion, presumably due to low base level, may have removed records of the Early Weichselian in this area.

The Timan glaciation

Admittedly, the suggested glaciation across the Timan ridge (Fig. 9D) is controversial. All the evidence for the concept comes from areas west of the ridge (Houmark-Nielsen *et al.* 2001; Kjær *et al.* 2001, 2003), and only has further support in interpretation of data from the northern part of the ridge (Matoshko 1999). The data west of the ridge include a number of fabric and petrographic analyses, and a variety of small-scale deformations from a correlative till unit. As the interpretation of each data set is the same it suggests an ice movement from east-southeast towards west-northwest. Both the composite stratigraphy discussed above (Fig. 2) and the absolute chronology (Fig. 6B) indicates a Weichselian age for this till unit. The ice movement direction inferred from these sites west of the Timan ridge is incompatible with ice movement directions to be expected by any of the three known ice sheets that operated in the

area during the Weichselian. Several papers from the Timan ridge area infer ice movements from western towards eastern directions (e.g. Matveyeva 1967; Lavrov & Potapenko 1978, 2005), i.e. opposite to the directions we find west of the ridge. This flow pattern is mainly based on the occurrence of erratics from Karelian and Kola deposited by a Scandinavian Ice Sheet. However, tills and erratics are found east of the Weichselian maximum limit of the Scandinavian Ice Sheet (cf. reconstructions in Svendsen *et al.* 2004; Fig. 10), and must therefore be pre-Weichselian according to our current understanding. Accordingly, we see no conflict with the above data, but acknowledge that there is no known supporting evidence for the reconstructed glaciation (Fig. 9D) east of the ridge (Svendsen *et al.* 2004) or in lake cores at the ridge itself (Henriksen *et al.* 2003; pers. comm. 2006).

Therefore, we conclude that the least dramatic interpretation of the ice-flow data is the suggested ice cap centred on the Timan ridge (Fig. 9D). The configuration to the west is based on the known sites with east-west ice flow, whereas the eastern extent is an even more tentative suggestion based on the available material to the west. The ice cap existed *c.* 75-70 kyr BP (Fig. 8) and was separated in time from the first Weichselian glacial event (Fig. 8) as full interstadial conditions developed in the intervening period (Houmark-Nielsen *et al.* 2001).

During deglaciation, fluvial and glaciofluvial deposition prevailed in the Mezen Bay area and along the river Pyoza (Houmark-Nielsen *et al.* 2001; Kjær *et al.* 2003). Glaciolacustrine sediments on upper Pyoza were deposited during deglaciation of the Timan ice cap, as there is a gradual transition from the till to these sediments (Fig. 5B). The location of the sediments on upper Pyoza provides evidence of an almost complete wastage of the Timan ice cap. There is, however, no record of a transition into warmer interstadial conditions (Houmark-Nielsen *et al.* 2001).

Barents Sea-dominated glaciation and White Sea Lake, c. 70-65 kyr

Subsequent to deglaciation of the Timan ice cap, glaciers moved into the area from the northwest (Fig. 8). The extent of this glaciation (Fig. 9E) is based on the end moraine belt along the Pyoza river that can be correlated with a till bed showing ice movements from the northwest (Houmark-Nielsen *et al.* 2001) and moraines pushed up at the western flank of the Timan ridge (Kjær *et al.* 2006). The Syurzi Moraines to the south of river Pyoza (Lavrov 1975) may represent the maximum stage of this glaciation, but this has yet to be confirmed by stratigraphical data; indeed the few luminescence dates available may suggest that it is pre-Weichselian. If the Syurzi Moraines represent the maximum of this glacial event, the moraines along the river Pyoza likely represent a recessional stage. Nevertheless, this glacial event represents the maximum southern extent of Weichselian glaciations in the eastern parts of our study area, a contention supported by the high sea level that followed deglaciation (Fig. 11).

Astakhov *et al.* (1999), and later Houmark-Nielsen *et al.* (2001) and Svendsen *et al.* (2004), correlated the Pyoza Moraines west of Timan with the Markhida Moraines east of Timan, suggesting they were formed during one ice advance. However, Kjær *et al.* (2006) were able to show that different segments of the end moraine complexes are deposited by two different ice advances, the oldest from the NW and the youngest from NE separated by marine, tidal sediments. The further eastwards continuation in the Kara Sea is problematic as pointed out by Svendsen *et al.* (2004). In this area we have merely indicated an ice margin between Novaya Zemlja and mainland Russia as was also done by Mangerud *et al.* (2004), cf. Fig. 10B.

The ice-movement directions show an ice sheet centred over the Barents Sea area (Kjær *et al.* 2006) that coalesced with ice over Scandinavia (Fig. 9E). A consequence would be that a lake formed in the White Sea basin south of this ice margin (the "White Sea Lake", Fig. 9E). This has yet to be demonstrated as no correlative lake sediments are found. This lake

might have drained towards the east via the Tsilma pass-point (Fig. 9E), and indeed a narrow channel cut into the pass is interpreted to have formed by drainage from the west (Nikolskaya *et al.* 2002). Moreover, a blackish clay on the Sula river, east of this pass, dated to 74-53 kyr might have been deposited in a lower lake at this time (Mangerud *et al.* 1999), or alternatively it may belong to a lake in Pechora during the next glacial stage (see below). Alternatively the lake might have drained towards the southwest via Lake Onega to the Baltic. If the Syurzi Moraines (Lavrov 1975, 1977, 1991) represent the maximum of this glacial event, the lake must have been dammed up to an elevation of 145 metres in the Mezen river basin (Lavrov 1975; Demidov *et al.* 2004). Under this scenario, the Tsilma pass-point would have opened as the ice retreated to the north.

The Mezen Interstadial, c. 65-55 kyr BP

The Barents Sea dominated ice sheet probably collapsed rapidly due to sea-level rise (Kjær *et al.* 2006), the White Sea Lake drained, and marine inundation followed, probably up to 40-50 metres above present sea level (Fig. 9F; Kjær *et al.* 2003; Jensen *et al.* 2006). This is the only recorded Weichselian high sea-level stand, the reason probably being that it occurred after rapid collapse of the maximum glaciation in the area. Palaeoecological information is sparse from this unit, but a sub-arctic climate somewhat more severe than today is indicated (Jensen *et al.* 2006). This reconstruction infers that river flow was towards the north as is shown from the Severnaya Dvina area. The marine unit shows a regression at least down to present sea level, only interrupted by a small transgression, before the area was glaciated again (Fig. 11; Jensen *et al.* 2006; Kjær *et al.* 2006).

Kara Sea dominated glaciation, c. 55-45 kyr BP, and the following long, ice-free period

Ice-flow during this glacial event (Fig. 8) was from the northeast, and the extent of the glaciation in the region is indicated by lobe shaped end-moraine systems north of the Pyoza Moraine and by the extent of till deposited from the same direction that occurs above tidal sediments (Kjær *et al.* 2006; Fig. 9G). In the Severnaya Dvina river basin, northbound fluvial drainage prevailed suggesting that the mouth of the White Sea was not blocked. Ice wedge casts in the fluvial sediments bears witness to periglacial conditions distally of the ice margin.

Stratigraphical and morphological data, including ice-flow indicators (Kjær *et al.* 2006), suggests that this event should be correlated with the Markhida Moraine at Markhida (Svendsen *et al.* 2004). This indicates that at least in some parts east of the Timan ridge, this ice advance was farther to the south than during the previous glaciation, and that a lake might have formed again in the Pechora basin with overflow to the Mezen drainage basin, and continuing to the north between the ice sheets (Fig. 9G). However, supporting evidence from this suggestion is not found in the Pechora basin (Mangerud *et al.* 2004). The ice extent further to the east cannot be resolved and is only tentatively indicated (Fig. 10C).

Apart from some evidence along the river Severnaya Dvina, the Kuloi coast and the Timan ridge area, there is little record of the period between the Kara Sea-dominated glaciation and the subsequent Scandinavian-dominated glaciation (Fig. 9G, H). The reason for this might be that sea level was low for a long period (Fig. 11), resulting in dominantly river incision (Jensen 2005). Severe climate conditions are indicated by presence of ice wedge casts. Fluvial sediments show northbound drainage, except just below the Scandinavian till along the river Severnaya Dvina where drainage was directed southwards (Fig. 8; Larsen *et al.* 1999; Lyså *et al.* 2001) due to damming by the approaching Scandinavian glacier.

The Scandinavian glacial maximum, c. 20 kyr BP, and the deglaciation

The maximum extent of the Scandinavian glaciation is well established in the Vaga and Severnaya Dvina areas (Fig. 9I; Larsen *et al.* 1999; Demidov *et al.* 2004; Demidov *et al.* 2006). The extent in the Mezen/Kuloi area is more dubious, and based on discontinuous ridges and topographical considerations (Demidov *et al.* 2006). The easternmost sites with Scandinavian till are at Cape Kargovsky on the Kuloi coast (Kjær *et al.* 2003), and at Tarkhanov on northwestern Kanin Peninsula (Demidov *et al.* 2006). Frequently a loosely compacted diamicton containing crystalline pebbles occurs along the western Kanin Peninsula suggesting proximity to the ice margin. The ice-marginal position along northern Kanin Peninsula is based on ice-proximal lake sediments that are capped by till at Madakha and Oiva (Kjær *et al.* 2006; Jensen *et al.* 2005). Lake sediments with OSL dates suggesting deposition some time after the previous Kara Sea-dominated advance is reported from the Timan coast (Mangerud *et al.* 1999). Subaerial exposure before deposition of the lake sediments (Mangerud *et al.* 1999) suggests that these are not to be linked with deglaciation, but rather a later advance. Accordingly, the Late Weichselian ice margin is drawn closer to the present coast in the Kanin – Timan area than in earlier reconstructions (Fig. 9I). Apart from these changes, the ice sheet configuration (Fig. 10D) is according to Svendsen *et al.* (2004).

The maximum position was reached some 20 to 17 kyr BP in the Dvina – western Kanin area (Larsen *et al.* 1999; Demidov *et al.* 2006; Linge *et al.* 2006b). Further east along the northern Kanin Peninsula there are no dates limiting the age of the maximum extent. However, from the Timan coast section (Mangerud *et al.* 1999), OSL dates suggest that the maximum extent was obtained between 19 and 32 kyr BP. No ice-dammed lakes comparable in size to the Early – Middle Weichselian lakes formed during this event (Mangerud *et al.* 2004) since the Barents and Kara ice sheets were located further north and did not block the

major rivers. In the Severnaya Dvina area, however, river drainage was re-routed by the Scandinavian Ice Sheet, via the Volga drainage system, and into the Caspian Sea (Kvasov 1979; Lunkka *et al.* 2001), and lower lakes draining northeastwards formed in front of lobes in the Kuloi and Mezen area (Demidov *et al.* 2006; Fig. 9I).

Deglaciation was initiated around 15 kyr BP (Fig. 8; Larsen *et al.* 1999; Demidov *et al.* 2006) and, as the Scandinavian Ice Sheet retreated westwards, it left vast areas covered with dead-ice and the northwards directed fluvial drainage was re-established (Lyså *et al.* 2001; Demidov *et al.* 2006). Two ice-marginal positions from the deglaciation period are mapped in the western part of the region (Demidov *et al.* 2006).

Wider implications

Four main sea level oscillations are recorded (Fig. 11): 1) A Saalian – Eemian regressive – transgressive – regressive sequence leaving marine sediments up to 140 m in the northern parts and more than 60 m in the south (Grøsfjeld *et al.* 2006; Lambeck *et al.* 2006); 2) an Early Weichselian sea level lower than present (Larsen *et al.* 2006); 3) a Middle Weichselian deglacial flooding and isostatic emergence, interrupted by a short lasting transgression (Jensen *et al.* 2006), and 4) a Late Weichselian regressive – transgressive cycle below present sea level (Gataullin *et al.* 2001). The most striking feature of the relative sea level changes is the amplitude of the glacial/interglacial response, the Saalian - Eemian being dominated by isostatic emergence up to more than 140 m above present sea-level, while the Weichselian - Holocene was dominated by eustatic sea level rise up to the present level (Fig. 11). Since the eustatic sea level rise in both periods is of the same order of magnitude, the difference lies in the more extensive Saalian ice cover over this region. The sea-level response during the Mezen Interstadial reflects rapid ice sheet collapse and deglacial flooding followed by

isostatic emergence, which, briefly, was overtaken by eustatic sea level rise (Fig. 11). Our field observations indicate that there was only short time between the deglaciation of the Timan ice cap and the subsequent Barents Sea-dominated glaciation (Fig. 8). Thus, it is speculated that the recorded isostatic uplift in the Middle Weichselian was a combined effect of the two glaciations (Fig. 11).

In Fig. 12 three Weichselian glaciation curves are presented, each oriented to represent dominance of the Kara Sea, the Barents Sea and the Scandinavian ice sheet, respectively. The Kara and Barents curves are predominantly constructed by data from Russia, i.e. around the maximum positions of any of the glaciations. Conversely, the Scandinavian curve (Olsen 1988; Larsen *et al.* 1999) is largely constructed by data from northern Scandinavia, i.e. far from any maximum position. Thus, the former two curves are more sensitive to large-scale glacial events, whereas the latter is more sensitive to deglaciations. The curves illustrate variations in time and space between the three dominant ice centres, and also why detailed correspondence between any of the curves and the modelled Eurasian ice volume variations (Lambeck *et al.* 2006; Fig. 12) should not be expected.

The IRD and melt-water signals appear to be very different in the NW Barents Sea and the East Arctic Ocean (Fig. 12), likely reflecting both different sources areas and complex transmittance of the signals in the ocean. The last deglaciation and IRD/melt-water events can be linked chronologically. In the Early to Middle Weichselian there is an approximate correspondence between IRD/melt-water events and the three main glaciations. The two younger of these, SP 6 and SP 8, may correspond to IRD/meltwater events in the Arctic Ocean dated to about 80 and 50 kyr. Allowing for uncertainties associated with dates, a melt water event in the Arctic Ocean around 59-55 kyr (Nørgaard-Pedersen *et al.* 1998) may correlate to the drainage of the White Sea Lake. Svendsen *et al.* (2004) and Mangerud *et al.* (2004), suggests that the IRD and melt-water signal at *c.* 50 kyr in the Arctic Ocean was

caused by deglaciation over the Taimyr Peninsula and drainage of large Siberian lakes. This may well be the case, and implies that the IRD signals at around 50 and 45 kyr BP in the Barents Sea broadly corresponds to the same deglaciation that followed the Kara Sea-dominated glaciation (Figs 10C, 12; SP 8).

The modelled volumetric changes (Fig. 12) only in gross terms reflect the ice sheet reconstructions of Svendsen *et al.* (2004) and that presented herein (Fig. 10). This may in part be due to regional variations in glacial history suggesting that the three ice centres counteracted each other in terms of total volume. Thus, apart from the signals representing the last glacial maximum, which can be confidentially tied to all records, correlations in detail are rather speculative. The Mezen Interstadial (MI) sea-level event occurring between glaciations SP 6 and SP 8 is well dated to 65-55 kyr BP (Kjær *et al.* 2003; Jensen *et al.* 2006) and corresponds to the minimum modelled Eurasian ice volume at *c.* 60 kyr (Fig. 12) as both are linked through the same eustatic signal. The re-growth of glaciers, in the Arkhangelsk region recorded as the Kara Sea-dominated glaciation (SP 8), is detected by increasing ice volume, but not to a uniquely distinct peak (Fig. 12). According to the ice volume curve, glaciers should, after this time, remain relatively stable or counterbalance each other until the final growth towards the last glacial maximum. This is not in line with our results presented herein (cf. Fig. 9H), and reconstructions from northern Scandinavia that suggest large ice-free areas 40-30 kyr BP (e.g. Olsen *et al.* 1996; Helmens *et al.* 2000).

Both Svendsen *et al.* (2004), and the model presented as Fig. 10 predicts that ice extent was most pronounced in the Kara Sea during the Early Weichselian, shifting towards the Barents Sea and Scandinavia during the Middle and Late Weichselian. The east-west migration might be explained by Atlantic moisture reaching far to the east during the Early Weichselian initiation phases, and progressively moving towards the source of precipitation as warmer-water fronts shifted southwards during ice build-up over the Barents Sea shelf. In

our reconstruction there is a large-scale deglaciation after the Barents Sea-dominated glaciation (Fig. 10B) before re-growth to a dominant Kara Sea glaciation (Fig. 10C). Kjær *et al.* (2006), suggested that the secondary pattern to the general east-to-west glacial migration was a response to rapid eustatic sea-level rise that caused glacier down-draw and collapse over the Barents Sea. This again would have triggered an outburst of the White Sea Lake into the Barents Sea (Fig. 9E). This possible chain of events, and in general the outlined dynamic glaciation history (Figs 10, 12), points towards instable shelf-centred ice sheets probably linked dynamically to sea level by large ice streams (e.g. Stokes & Clark 2001).

Conclusions

During the Weichselian all three Eurasian ice sheets – the Kara Sea, the Barents Sea and the Scandinavian – terminated in the Arkhangelsk region of NW Russia. The record demonstrates a dynamical glacier system, generally supporting an east-to-west migration over time in main glacier activity (Siegert *et al.* 2001; Svendsen *et al.* 2004), but it also shows a Middle Weichselian return to an easterly-centred glaciation before the final Scandinavian-dominated glaciation during the Late Weichselian global glacial maximum. The main events can be summarized as follows:

- The coastline during the maximum early Eemian sea-level high-stand was situated c. 350 km inland of the present. Sea level reached at least 60 m above present in the southern part of the region, and at more than 140 m in the northernmost parts. This reflects the difference in isostatic emergence associated with the preceding Saalian ice sheet. In the late Eemian – Early Weichselian transition sea level dropped below present (Larsen *et al.* 2006).

- At *c.* 100-90 kyr BP the north-eastern parts of the area was glaciated by an easterly (Kara Sea) dominated ice sheet. This corresponds to the Weichselian maximum glaciation in the east (Svendsen *et al.* 2004), and was associated with the damming of the Lake Komi in the Pechora lowlands east of the Arkhangelsk region (Mangerud *et al.* 2004). The limited extent of the Scandinavian- and the Kara Sea-dominated ice sheets means that the two did not merge, and no lake corresponding to Lake Komi formed in the White Sea basin. The Komi Lake had the outlet across the Timan ridge, draining towards the north between the Kanin and Kola peninsulas into the Barents Sea. Following deglaciation, full interstadial conditions developed that lasted until *c.* 75 kyr BP.
- West of the Timan ridge, the regional distribution of a till bed dated to between 75 and 70 kyr and with ice flow directions from east-southeast, indicates that a local ice cap developed over the Timan ridge (Houmark-Nielsen *et al.* 2001; Kjær *et al.* 2003). The eastern extent of this ice cap in the Pechora area close to the Timan ridge has not yet been found (Svendsen *et al.* 2004).
- Shortly after deglaciation of the Timan ice cap, between some 70 and 65 kyr BP, the Arkhangelsk region was invaded by a Barents Sea-dominated glaciation that moved into the area from the northwest. It is probable that the glaciers merged with the Scandinavian Ice Sheet. One inference from this is that an ice-dammed lake formed in the White Sea basin, but sediments deposited in this lake have not yet been found. The outlet for this lake was either across the Timan ridge to the Pechora lowlands or via lake Onega to the Baltic.
- Subsequent to collapse of the Barents Sea Ice Sheet the area was inundated by the sea up to 40-50 m above present sea level (Jensen *et al.* 2006; Kjær *et al.* 2006). Although

sparse, the faunal evidence from the shallow marine sediments suggests sub-arctic, normal marine conditions (Jensen *et al.* 2006).

- Between *c.* 55 and 45 kyr BP, the north-eastern part of the area was glaciated again, this time by glaciers moving from the northeast. Fluvial drainage along the river Severnaya Dvina was directed to the north indicating that there was open drainage towards the Barents Sea, and thus no coalescence with the Scandinavia Ice Sheet.
- A long interstadial (*c.* 45-20 kyr BP) was followed by the Scandinavian-dominated glaciation during the global glacial maximum. At *c.* 20 kyr BP this glaciation penetrated far up the Severnaya Dvina drainage basin and rerouted this river to the south via the river Volga (Kvasov 1979). The river Mezen was diverted to the northeast along the Timan coast by an ice margin situated just north of the present coast.
- The empirically reconstructed glacial evolution is largely in line with numerical modelling by Lambeck *et al.* (2006). Detailed correlations between on- and offshore records are to some degree hampered by insufficient dating control and lack of detailed knowledge on source-to-sink transmittance of glacial signals.

Acknowledgements. - This is a contribution to the European Science Foundation “QUEEN” program (Quaternary Environment of the Eurasian North) and the Norwegian Research Council "NORPAST" program (Past Climates of the Norwegian Region). The work was funded through the European Community project “Eurasian Ice Sheets” (contract ENV4-CT970563), the Norwegian Research Council, the Danish Natural Science Research Council (CLIENT and TrippleJunction projects), Norsk Hydro AS, the Swedish Polar Secretariat, The Norwegian Barents Secretariat, and the Swedish Crafoord Foundation. Luminescence dating was carried out at the Nordic Laboratory for Luminescence Dating, Risø, Denmark. Radiocarbon dating was obtained from the Trondheim (Norway) and the Aarhus (Denmark) laboratories. Samples for *in situ* cosmogenic ¹⁰Be surface exposure dating were processed at Washington State University, Vancouver (USA), and concentrations were measured at the Tandem AMS facility at Gif-sur-Yvette (France). Øystein Jæger, Geological Survey of Norway,

Dimitri Nokolaev and many other Russians assisted in the field. Irene Lundquist, Geological Survey of Norway, assisted with some of the figures. Discussions with colleagues from the QUEEN project contributed significantly to the work. Jochen Knies, Geological Survey of Norway read part of the manuscript critically. Valery Astakhov, St. Petersburg University and one anonymous reviewer made very constructive comments to the manuscript.

References

- Arkhipov, S.A., Ehlers, J., Johnson, R.G. & Wright, H.E., Jr. 1995: Glacial drainage towards the Mediterranean during the Middle and Late Pleistocene. *Boreas* 24, 196-206.
- Astakhov, V. 2004: Middle Pleistocene glaciations of the Russian North. *Quaternary Science Reviews* 23, 1285-1311.
- Astakhov, V.I., Svendsen, J.I., Matiouchkov, A., Mangerud, J., Maslenikova, O. & Tveranger, J. 1999: Marginal formations of the last Kara and Barents ice sheets in northern European Russia. *Boreas* 28, 23-45.
- Biske, G.S. & Devyatova, E.I. 1965: Pleistocene transgression in the north of Europe: Antropogene of the Arctic and Sub-Arctic regions. VIIth Session of INQUA, Trudy Institute of the Geology of the Arctic, Moscow, *Nedra* 43, 155-176. (In Russian).
- Bronk, R.C. 2001: Development of the Radiocarbon Program OxCal, *Radiocarbon*, 43, 355-363.
- Bronk, R.C. 1995: Radiocarbon Calibration and Analysis of Stratigraphy: The OxCal Program *Radiocarbon* 37, 425-430.
- Chebotareva, N.S. (ed.) 1977: *Structure and dynamics of the last ice sheet of Europe*, 143 pp. Nauka, Moscow. (In Russian).
- De Geer, G. 1896: *Om Skandinaviens Geografiska Utveckling efter Istiden*. 160 pp. Nordstedt & Söner, Stockholm.

Demidov, I.N., Houmark-Nielsen, M., Kjær, K.H. & Larsen, E. 2006: The Last Scandinavian Ice Sheet in northern Russia: ice flow patterns and decay dynamics. *Boreas*, this issue.

Demidov, I.N., Houmark-Nielsen, M., Kjær, K.H., Larsen, E., Lyså, A., Funder, S., Lunkka, J.-P. & Saarnisto, M. 2004: Valdaian glacial maxima in the Arkhangelsk district of Northwest Russia: a review. In Ehlers, J. & Gibbard, P.L. (eds.): *Quaternary Glaciations - Extent and Chronology. Part I: Europe*, 321-326. Elsevier, Amsterdam.

Devyatova, E.I. 1982: *Late Pleistocene environments as related to human migrations in the Dvina river basin and in Karelia*. 156 pp. Karelia, Petrozavodsk. (In Russian).

Eyles, N., Eyles, C.H. & Miall, A.D. 1983: Lithofacies types and vertical profile models; an alternative approach to the description and environmental interpretation of glacial diamict and diamictite sequences. *Sedimentology* 30, 395-410.

Funder, S., Demidov, I. & Yelovicheva, Y. 2002: Eemian mollusc faunas and hydrography of the Baltic and the White Sea – North Sea seaway. *Palaeogeography, Palaeoclimatology, Palaeoecology* 184, 275-304.

Gataullin, V., Mangerud, J. & Svendsen, J.I. 2001: The extent of the Late Weichselian ice sheet in the southeastern Barents Sea. *Global and Planetary Change* 31, 453-474.

Grøsfjeld, K., Funder, S., Seidenkrantz, M-S. & Glaister, C. 2006: Last interglacial marine environments in the White Sea region, northern Russia. *Boreas*, this issue.

Grosswald, M.G. 1980: Late Weichselian Ice Sheets of Northern Eurasia. *Quaternary Research* 13, 1-32.

Grosswald, M.G. 1998: Late-Weichselian ice sheets in Arctic and Pacific Siberia. *Quaternary International* 45/46, 3-18.

- Hampson, G.J. & Storms, J.E.A. 2003: Geomorphological and sequence stratigraphic variability in wave-dominated, shoreface-shelf parasequences. *Sedimentology* 50, 667-701.
- Helmens, K. F., Räsänen, M. E., Johansson, P. W., Jungner, H. & Korjonen, K. 2000: The Last Interglacial – Glacial cycle in NE Fennoscandia: a nearly continuous record from Sokli (Finnish Lapland). *Quaternary Science Reviews* 19, 1605- 1623.
- Henriksen, M., Mangerud, J., Paus, A. & Svendsen, J.I. 2003: Late Pleistocene record from Lake Yamozero, Timan Ridge, northern Russia, 34 pp. In Henriksen, M.: *Late Pleistocene stratigraphy of the Pechora Region, Arctic Russia*. Ph.D. dissertation, University of Bergen.
- Houmark-Nielsen M., Demidov, I., Funder, S., Grøsfjeld, K., Kjær, K.H., Larsen, E., Lavrova, N., Lyså, A. & Nielsen, J.K. 2001: Early and Middle Weichselian terrestrial and marine-based glaciations and periglacial interstadials in northwest Russia: New evidence from the Pjoza River area. *Global and Planetary Change* 31, 213-235.
- Jensen, M. 2005: Fluvial response to climate and sea level change in multistorey valley fill during the last interglacial – glacial cycle, Arkhangelsk region, NW Russia, 25 pp. In Jensen, M.: *Sedimentary response to Quaternary climate and sea level change: examples from the last glacial cycle, Arkhangelsk region, NW Russia*. Ph.D. dissertation, University of Copenhagen.
- Jensen, M., Larsen, E., Demidov, I., Funder, S. & Kjær, K.H. 2006: Middle Weichselian shallow-marine sediments in the Arkhangelsk Region, NW Russia; Sea level change and relation to north Eurasian glaciations. *Boreas*, this issue.
- Jensen, M., Larsen, E., Demidov, I. & Kjær, K.H. 2005: Facies architecture in multistorey glacio-lacustrine basins, Northern Kanin Peninsula, NW Russia 38 pp. In Jensen,

M.: *Sedimentary response to Quaternary climate and sea level change: examples from the last glacial cycle, Arkhangelsk region, NW Russia*. Ph.D. dissertation, University of Copenhagen.

Kjær, K.H., Demidov, I., Houmark-Nielsen, M. & Larsen, E. 2001: Distinguishing between tills from Valdaian ice sheets in the Arkhangelsk region, Northwest Russia. *Global and Planetary Change* 31, 199-212.

Kjær, K.H., Demidov, I.N., Larsen, E., Murray, A. & Nielsen, J.K. 2003: Mezen Bay – a key area for understanding Weichselian glaciations in northern Russia. *Journal of Quaternary Science* 18, 73-93.

Kjær, K.H., Larsen, E., Funder, S., Demidov, I., Jensen, M. & Håkansson, L. 2006: Eurasian ice sheet interaction in Northern Russia throughout the late Quaternary. *Boreas*, this issue.

Korchagin, A.A. 1937: On endmoraine landscapes of river Mezen. *Izvestia geograficheskoga obschestva* 69, 623-631. (in Russian).

Krasnov, I.I., Duphorn, K. & Voges, A. 1971: *International Quaternary Map of Europe, Sheet 3: Nordkapp*. INQUA commission. Bundesanstalt für Bodenforschung, Hannover.

Krüger, J. & Kjær, K.H. 1999: A data chart for field description and genetic interpretation of glacial diamicts and associated sediments – with examples from Greenland, Iceland, and Denmark. *Boreas* 28, 386-402.

Kvasov, D.D. 1979: Late-Quaternary history of large lakes and inland seas of eastern Europe. *Annales Academiae Scientiarum Fennicae AIII*, 1-71.

Lambeck, K., Purcell, A., Funder, S., Kjær, K., Larsen, E. & Möller, P. 2006: Constraints on the Late Saalian to early Middle Weichselian ice sheet of Eurasia from field data and rebound modelling. *Boreas*, this issue.

- Landvik, J.Y., Bondevik, S., Elverhøi, A., Fjeldskaar, W., Mangerud, J., Salvigsen, O., Siegert, M.J., Svendsen, J.I. & Vorren, T.O., 1998: The last glacial maximum of Svalbard and the Barents Sea area: ice sheet extent and configuration. *Quaternary Science Reviews* 17, 43-75.
- Larsen, E., Kjær, K.H., Jensen, M., Demidov, I., Håkansson, L. & Paus, Aa. 2006: Early Weichselian palaeoenvironments reconstructed from a mega-scale thrust-fault complex, Kanin Peninsula, NW Russia. *Boreas*, this issue.
- Larsen, E., Lyså, A., Demidov, I., Funder, S., Houmark-Nielsen, M., Kjær, K.H. & Murray, A.S. 1999: Age and extent of the Scandinavian ice sheet in northwest Russia. *Boreas* 28, 115-132.
- Lavrov, A.S. 1975: Late Pleistocene impounded lakes in the North-East of the Russian Plain. *IV All-Union symposium on history of lakes, v. 2*, 119-127. Leningrad.
- Lavrov, A.S. 1977: Kola-Mezen, Barents Sea-Pechora, Novaya Zemlya-Kolva ice streams. In Chebotareva, N.S. (ed.): *The structure and Dynamics of the Last Ice Sheet of Europe*, 83-100. Nauka, Moscow (in Russian).
- Lavrov, A.S. 1991: *Map of Quaternary deposits. Sheet Mezen Scale 1:1000 000*. VSEGEI, Leningrad (in Russian).
- Lavrov, A.S. & Potapenko, L.M. 1978: Coarse-clastic material of ground moraines of the West Timan region: composition and regularities of formation. In Shantser, E.V. & Lavrushin, Yu.A. (eds.): *Ground moraines of continental glaciations*. Geological Institute of Academy of Science USSR, Moscow, 216-232.
- Lavrov, A.S. & Potapenko, L.M. 2005: *Neopleistocene of the northeastern Russian Plain*. Aerogeologia, Moscow, 222 pp, 5 maps.
- Lavrushin, Yu. A. & Spiridonova, E.A. 1995: The Late Pleistocene events in the north of European Russia: Geology and palaeoenvironments. In Velichko, A.A. (ed.): *Climate*

and environment changes of east Europe during Holocene and late-Middle Pleistocene, 63-68. IGU conference on Global changes and geography. Moscow, August 14-18, 1995.

Linge, H., Brook, E.J., Nesje, A., Raisbeck, G.M., Yiou, F. & Clark, H. 2006a: In situ ^{10}Be exposure ages from southeastern Norway: Implications for the geometry of the Weichselian ice sheet. *Quaternary Science Reviews*, in press.

Linge, H., Larsen, E., Kjær, K.H., Demidov, I., Brook, E.J., Raisbeck, G.M. & Yiou, F. 2006b: Cosmogenic ^{10}Be exposure dating across Early to Late Weichselian ice-marginal zones in northern Russia. *Boreas*, this issue.

Lunkka, J.P., Saarnisto, M., Gey, V., Demidov, I. & Kiselova, V. 2001: Extent and age of the Last Glacial Maximum in the southeastern sector of the Scandinavian Ice Sheet. *Global and Planetary Change* 31, 407-425.

Lyså, A., Demidov, I., Houmark-Nielsen, M. & Larsen E. 2001: Late Pleistocene stratigraphy and sedimentary environment of the Arkhangelsk area, Northwest Russia. *Global and Planetary Change* 31, 179-199.

Mangerud, J., Astakhov, V.I., Murray, A. & Svendsen, J.I.. 2001: The chronology of a large ice-dammed lake and Barents-Kara Ice Sheet advances in Northern Russia. *Global and Planetary Change* 31, 321-336.

Mangerud, J., Jakobsson, M., Alexanderson, H., Astakhov, V., Clarke, G.K.C., Henriksen, M., Hjort, C., Krinner, G., Lunkka, J.P., Möller, P., Murray, A., Nikolskaya, O., Saarnisto, M. & Svendsen, J.I. 2004: Ice-dammed lakes and rerouting of the drainage of northern Eurasia during the last Glaciation. *Quaternary Science Reviews* 23, 1313-1332.

Mangerud, J., Svendsen, J.I. & Astakhov, V.I. 1999: Age and extent of the Barents and Kara Sea sheets in Northern Russia. *Boreas* 28, 46-80.

- Masarik, J., Frank, M., Schäfer, J.M. & Wieler, R. 2001: Correction of in situ cosmogenic nuclide production rates for geomagnetic field intensity variations during the past 800,000 years. *Geochimica et Cosmochimica Acta* 65, 2995-3003.
- Maslenikova, O. & Mangerud, J. 2001: Where was the outlet of the ice-dammed Lake Komi. Northern Russia? *Global and Planetary Change* 31, 337-345.
- Matoshko, A.V. 1999: Quaternary glacial deposits and landforms of the north Timan region, Russia – a possible center of local glaciation. *Geological Society of America Special Paper* 337, 179-185.
- Matveyeva, G.V. 1967: Results of a glacial pebbles study in the Middle Timan. Bulletin *Komissii po izucheniyu chetvertichnogo perioda, Academy of Science USSR, Moscow* 9, 15-22.
- Merklin, R.L., Zarkhidze, V.S. & Ilina, L.B. 1979: Catalogue of Pliocene-Pleistocene marine molluscs from the NE European part of the USSR. *USSR Academy of Sciences. Transactions of Palaeontological Institute*, 173, 96 pp.
- Murray, A.S, Marten, R., Johnston, A. & Martin, P. 1987: Analysis for naturally occurring radionuclides at environmental concentrations by gamma spectrometry. *Journal of Radioanalytical and Nuclear Chemistry, Articles* 115, 263-288.
- Murray, A.S. & Wintle, A.G. 2000: Luminescence dating of quartz using an improved single aliquot regenerative-dose protocol. *Radiation Measurements* 32, 57-73.
- Nielsen, J.K. & Funder, S. 2003: Taphonomy of Eemian marine molluscs and acorn barnacles from eastern Arkhangelsk region, northern Russia. *Palaeogeography, Palaeoclimatology, Palaeoecology* 191, 139-168.
- Nikolskaya, O., Astakhov, V., Mangerud, J., Matiouchkov, A. & Svendsen, J.I. 2002: *Geomorphological map of the Pechora Basin and adjacent areas*. NIIKAM, St. Petersburg.

- Nio, S.-D. & Yang, C.-S. 1991: Diagnostic attributes of clastic tidal deposits: a review. In Smith, D.G., Reinson, G.E., Zaitlin, B.A. & Rahmani, R.A. (eds.): *Clastic tidal sedimentology. Canadian Society of Petroleum Geologists, Memoir 16*, 3-28.
- Nørgaard-Pedersen, N., Spielhagen, R.F., Thiede, J. & Kassens, H. 1998: Central Arctic surface ocean environment during the past 80,000 years. *Paleoceanography 13*, 193-204.
- Olley, J.M., Murray, A.S. & Roberst, R.G. 1996: The effects of disequilibria in uranium and thorium decay chains on burial dose rates in fluvial sediments. *Quaternary Geochronology 15*, 751-760.
- Olsen, L. 1988: Stadials and interstadials during the Weichsel glaciation on Finnmarksvidda, northern Norway. *Boreas 17*, 517-539.
- Olsen, L., Mejdahl, V. & Selvik, S.F. 1996: Middle and Late Pleistocene stratigraphy, chronology and glacial history in Finnmark, North Norway. *Norges geologiske undersøkelse Bulletin 429*, 1-111.
- Polyak, L., Gataullin, V., Okuneva, O. & Stelle, V. 2000: New constraints on the limits of the Barents-Kara ice sheet during the Last Glacial Maximum based on borehole stratigraphy from the Pechora Sea. *Geology 28*, 611-614.
- Raisbeck, G.M., Yiou, F., Bourlès, D., Brown, E., Deboffe, D., Jouhannau, P., Lestringuez, J. & Zhou, Z.Q. 1994: The AMS facility at Gif-sur-Yvette: progress perturbations and projects. *Nuclear Instruments and Methods in Physics Research B 92*, 43-46.
- Ramsay, W. 1904: Beiträge zur Geologie der recenten und pleistocänen Bildungen der Halbinsel Kanin. *Bulletin de Société de Géographie de Finlande, Fennia 21*, 1-66.
- Reimer, P.J., Baillie, M.G.L., Bard, E., Bayliss, A., Beck, J.W., Bertrand, C.J.H., Blackwell, P.G., Buck, C.E., Burr, G.S., Cutler, K.B., Damon, P.E., Edwards, R.L., Fairbanks, R.G., Friedrich, M., Guilderson, T.P., Hogg, A.G., Hughen, K.A., Kromer, B.,

- McCormac, G., Manning, S., Bronk Ramsey, C., Reimer, R.W., Remmele, S., Southon, J.R., Stuiver, M., Talamo, S., Taylor, F.W., van der Plicht, J. & Weyhenmeyer, C.E. 2004: IntCal04 Terrestrial Radiocarbon Age Calibration, 0 - 26 ka cal BP. *Radiocarbon*, 46, 1029-1058.
- Siegert, M., Dowdeswell, J.A. Hald, M. & Svendsen, J.I. 2001: Modelling the Eurasian Ice Sheet through a full (Weichselian) glacial cycle. *Global and Planetary Change* 31, 367-385.
- Spielhagen, R.F., Baumann, K.H., Erlenkeuser, H., Frederichs, T., Nowaczyk, N.R., Nørgaard-Pedersen, N., Thiede, J., Vogt, C. & Weiel, D. 2004: Arctic Ocean deep-sea record of northern Eurasian ice sheet history. *Quaternary Science Reviews* 23, 1455-1483.
- Stokes, C.R. & Clark, C.D. 2001: Palaeo-ice streams. *Quaternary Science Reviews* 20, 1437-1457.
- Stone, J.O. 2000: Air pressure and cosmogenic isotope production. *Journal of Geophysical Research* 105, 23,752-23,759.
- Svendsen, J.I., Alexanderson, H., Astakhov, V.I., Demidov, I., Dowdeswell, J.A., Funder, S., Gataullin, V., Henriksen, M., Hjort, C., Houmark-Nielsen, M., Hubberten, H.W., Ingólfsson, Ó., Jakobsson, M., Kjær, K.H., Larsen, E., Lokrantz, H., Lunkka, J.P., Lyså, A., Mangerud, J., Matioushkov, A., Murray, A., Möller, P., Niessen, F., Nikolskaya, O., Polyak, L., Saarnisto, M., Siegert, C., Siegert, M.J., Spielhagen, R.F. & Stein, R. 2004: Late Quaternary ice sheet history of northern Eurasia. *Quaternary Science Reviews* 23, 1229-1271.
- Svendsen, J.I., Astakhov, V.I., Bolshiyakov, D.Yu., Demidov, I., Dowdeswell, J.A., Gataullin, V., Hjort, C., Hubberten, H.W., Larsen, E., Mangerud, J., Melles, M., Möller, P., Saarnisto, M. & Siegert, M.J. 1999: Maximum extent of the Eurasian ice

sheets in the Barents and Kara Sea region during the Weichselian. *Boreas* 28, 234-242.

Thomas, P.J., Murray, A.S., Kjær, K.H., Funder, S., & Larsen, E. 2006: Optically stimulated luminescence dating of glacial sediments from Arctic Russia – depositional bleaching and methodological aspects. *Boreas*, this issue.

Velichko, A.A. 1995: The Pleistocene termination in northern Eurasia. *Quaternary International* 28, 105-111.

Velichko, A.A., Kononov, Yu.M. & Faustova, M.A. 1997: The last glaciation on the earth: size and volume of ice-sheets. *Quaternary International* 41/42, 43-51.

Waelbroeck, C., Labeyrie, L., Michel, E., Duplessy, J.C., McManus, J.F., Lambeck, K., Balbon, E. & Labracherie, M. 2002: Sea-level and deep water temperature changes derived from benthic foraminifera isotopic records. *Quaternary Science Reviews* 21, 295–305.

Zharkidze, V.S. 1983: Complex of Neogene-Quaternary molluscs. In Gramberg I.S & Kulakov, I.N (eds.): *Main problems of late Cenozoic palaeogeography of the Arctic*. Ministry of Geology of the USSR, 'SEVMORGEOLOGIYA', 190, 94-104.

Zharkidze, V.S. & Samoilovich, Yu.G. 1989: Late Cainozoic stratigraphy and palaeoceanography of the Barents Sea. In Herman, Y. (ed.): *The arctic seas, climatology, oceanography, geology and biology*, 721-729. Van Nostrand Reinhold Company, New York.

Figures

1. Study area with names used in the text. The locations of stratigraphical profiles, A-E (Fig. 3) is shown. Approximate positions of three end-moraine zones are stippled.
2. Stratigraphical scheme of the Arkhangelsk area for the Eemian to the Holocene. Each stratigraphical position represents either several parallel environments, e.g. marine and fluvial, or there is a time transgressive development, e.g. ice-proximal – sub-glacial – deglacial.
3. Stratigraphical profiles showing distribution of units correlated according to the stratigraphical scheme (Fig. 2). The profiles are shown on the map (Fig. 1). A: The Arkhangelsk – Severnaya Dvina – Vaga area is a northwards extension of the work presented by Lyså *et al.* (2001). B: The Morzhovets Island – Kuloi coast area. The Choshskaya Bay (C) and Kanin Peninsula areas (D) are based on Kjær *et al.* (2006). The Timan beach site in profile C is from Mangerud *et al.* (1999). E: The Mezen Bay – Pyoza area is an extension of work presented by Biske & Devyatova (1965), Houmark-Nielsen *et al.* (2001) and Kjær *et al.* (2003). The cited papers contain detailed descriptions and interpretations within the sub-regions.
4. A. Mollusc bearing, Eemian shore gravel c. 10 m above present sea level at Zaton on the river Mezen. B. Northern Kanin showing glaciotectonically thrust sand (SP 2) and *in situ* glaciolacustrine sediments (SP 10). Persons working in the section are encircled. C. Terraces developed in down-wasting complex (SP 3) at Pestsovaya on western Kanin Peninsula. D. The Pestsovaya Till at Pestsovaya with associated deglacial sediments.
5. A. Overview of the stratigraphy at Cape Tolstik. B. The Yolkino Till on upper river Pyoza with a gradual transition to deglacial glaciolacustrine sediment. C. Glaciotectonically folded (from NE) tidal sediments (Mezen Interstadial) at Bolshoi Vzglavnyie showing alternations between dark, clayey (winter?) and light, sandy

(summer?) sub-units. D. The bluish, fine-grained sediment in the middle shows two full tidal cycles within one of the fine-grained sub-units at Bolshoi Vzglavnyie. E. The Syomzha Till (SP 8) at Syomzha with rafts from underlying tidal sediments (SP 7). F. Fluvial sediments with erosive contact to underlying Eemian, marine sediments at the river Dvina. G. End moraine from the Scandinavian maximum glaciation at river Vaga. The ice-proximal slope is to the right. H. Glaciolacustrine sediments (SP 10) formed proximally to the ice margin during the Last Glacial Maximum, northern Kanin Peninsula.

6. Optically stimulated luminescence and radiocarbon dates plotted relative to the five regional till beds, SP 3, 5, 6, 8 and 10 (Fig. 2). The dated material is from non-glacial sediments below and above the respective till unit, and from proglacial or deglaciation sediments. The dates are listed in Tables 1 and 2.
7. Exposure age dating results (Linge *et al.* 2006b) in relation to the reconstructed ice limits (Fig. 10B, D, E, G, I) with ages based on OSL dating. Plain numbers are ages obtained on bedrock surfaces, underlined numbers are ages obtained on glacial erratic surfaces. The dates are listed in Table 3.
8. Event stratigraphic model for the Arkhangelsk region synchronising stratigraphies from the Severnaya Dvina – White Sea area (Larsen *et al.* 1999; Lyså *et al.* 2001; Demidov *et al.* 2006), the Mezen Bay – Pyoza area (Houmark-Nielsen *et al.* 2001; Kjær *et al.* 2003; Grøsfjeld *et al.* 2006), the Kanin area (Kjær *et al.* 2006; Larsen *et al.* 2006), and the Choshskaya Bay area (Jensen *et al.* 2006; Kjær *et al.* 2006).
9. Palaeogeographical reconstructions from the Arkhangelsk region showing nine time intervals (A-I) from the Eemian to the Late Weichselian. Transgression maxima are shown for A, the early Eemian (Funder *et al.* 2002) and F, the Mezen Interstadial (Jensen *et al.* 2006). For the others, when sea level is shown, eustatic sea level

according to Waelbroeck *et al.* (2002) is indicated without considering isostatic adjustments.

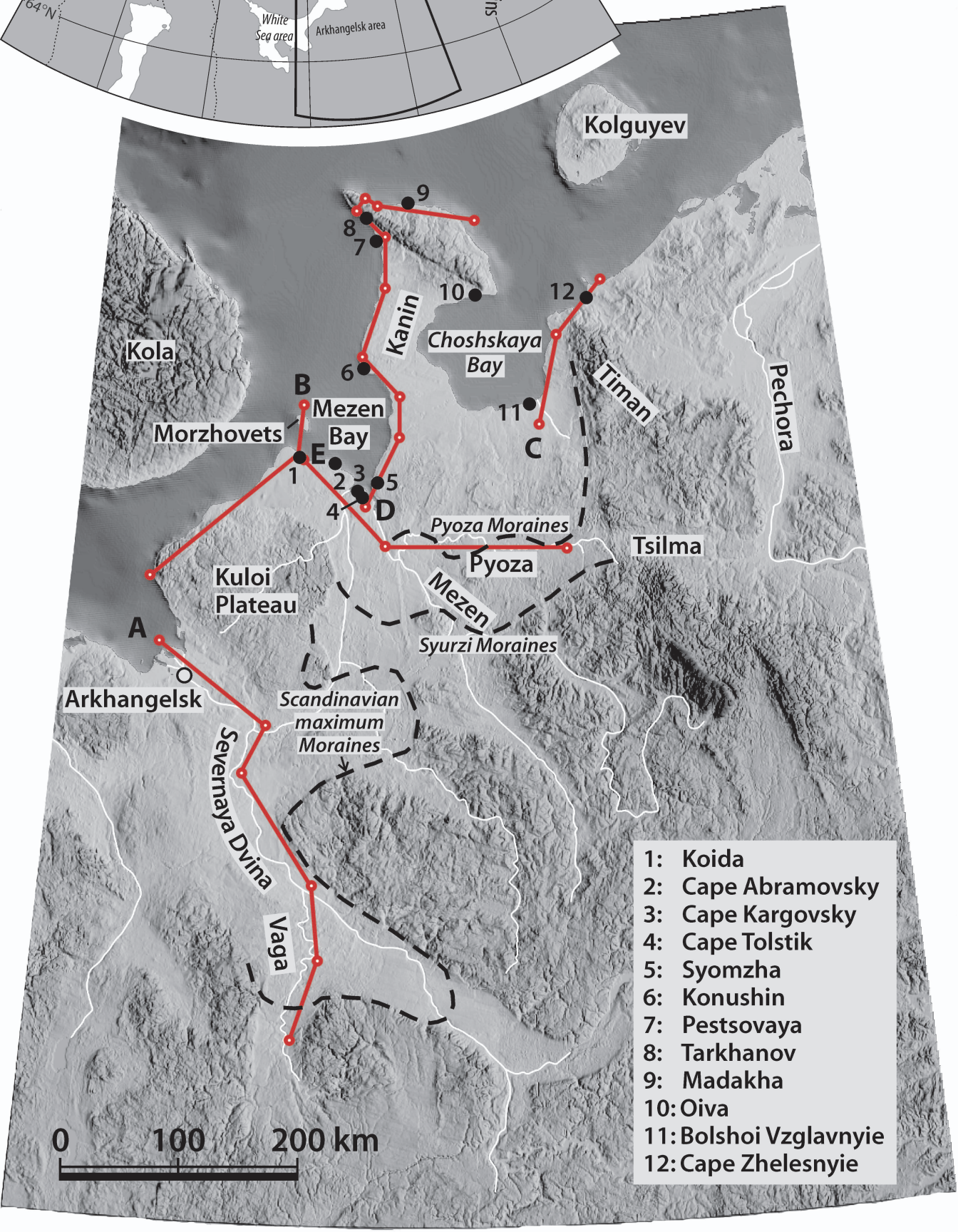
10. Reconstruction of Eurasian ice sheets: A. *c.* 100-90 kyr BP, B. *c.* 70-65 kyr BP, C. *c.* 55-45 kyr BP, and D. *c.* 20 kyr BP. Note that the chronologies applied are that developed in this paper (Fig. 6). Ice dammed lakes in front of the ice margins are not included (see Fig. 9). The reconstruction at *c.* 100-90 kyr (A) is according to Svendsen *et al.* (2004), except for the split between the ice sheets in the Barents Sea suggested from data in this paper. The ice sheets at *c.* 70-65 kyr BP (B) are largely according to the reconstruction of the Middle Weichselian by Svendsen *et al.* (2004), except for some differences in interpretations across the Timan ridge (Kjær *et al.* 2006). The reconstruction at *c.* 55-45 kyr BP (C) is based on the results in Kjær *et al.* (2006) and demonstrates a second Middle Weichselian glaciation, and the results from the Severnaya Dvina area showing fluvial drainage to the north (Lyså *et al.* 2001) suggesting that the Barents Sea was ice free. Allowing for the latter, the Scandinavian Ice Sheet is according to Svendsen *et al.* (2004). The ice extents at this time in the east and over the northern archipelagos are only tentative. The Last Glacial Maximum (D) is according to Svendsen *et al.* (2004) although there are some adjustments in the Kanin Peninsula area (Demidov *et al.* 2006).
11. A. Compilation of Saalian – Holocene relative sea level variations for the northernmost Arkhangelsk and Pechora coastal areas. The Saalian – Eemian is according to Grøsfjeld *et al.* (2006) and Lambeck *et al.* (2006), the Early Weichselian low-stand according to Larsen *et al.* (2006), the Mezen Interstadial according to Jensen *et al.* (2006), and the Late Weichselian – Holocene according to Gataullin *et al.* (2001). Also shown are periods of glaciations with stratigraphic positions according to Fig. 2. B. Eustatic sea level curve from Waelbroeck *et al.* (2002), and C, the resultant

isostatic curve when B is subtracted from A. Isostasy is not calculated for the Early Weichselian low-stand as the exact timing and sea-level are unknown.

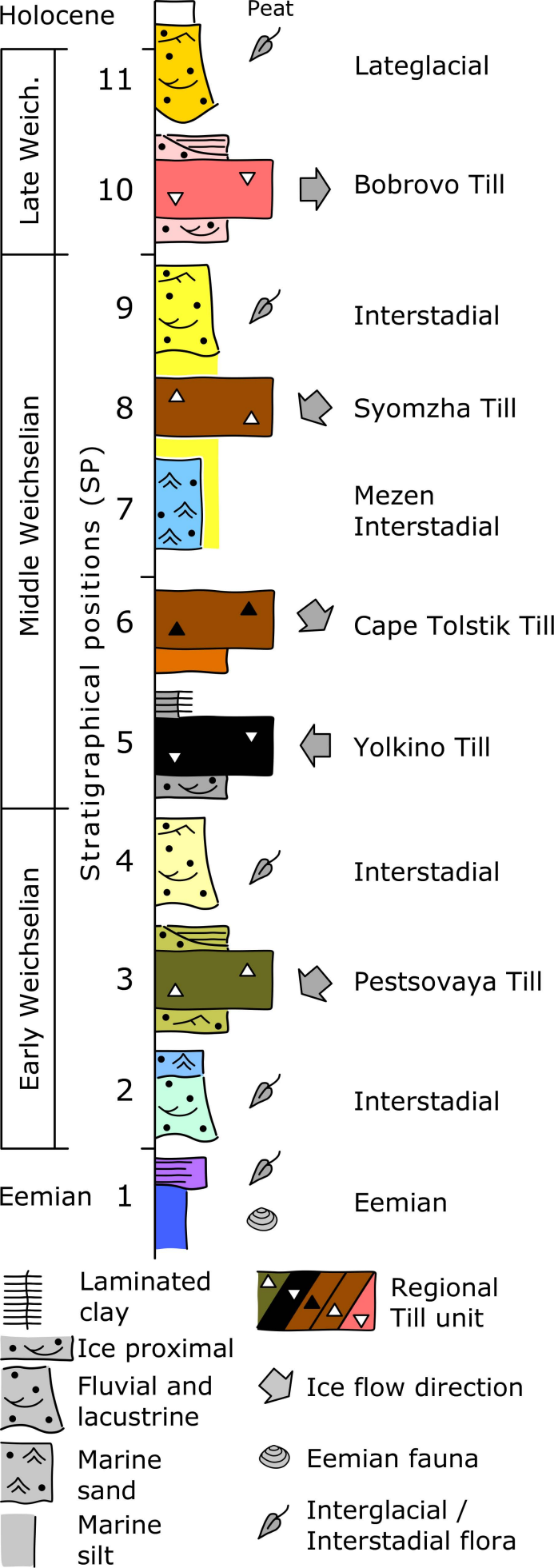
12. Weichselian glaciation curves depicting Scandinavian dominance (Olsen 1988; Larsen *et al.* 1999), Barents Sea dominance and Kara Sea dominance. Ice volumes from Lambeck *et al.* (2006). Ice rafted debris (IRD) and melt-water drainage events in the east to central Arctic Ocean from Spielhagen *et al.* (2004), and in the northwestern Barents Sea from Siegert *et al.* (2001).

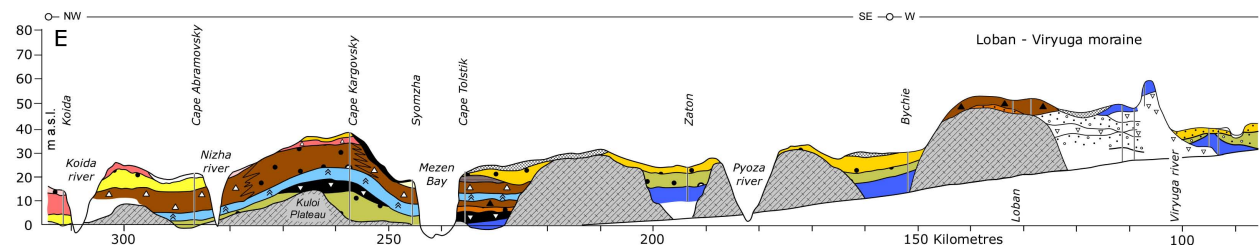
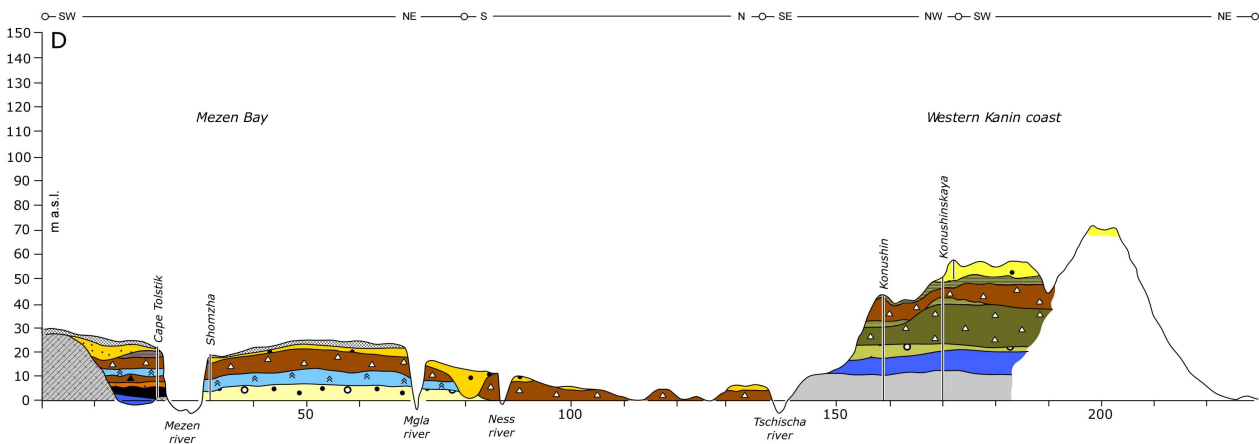
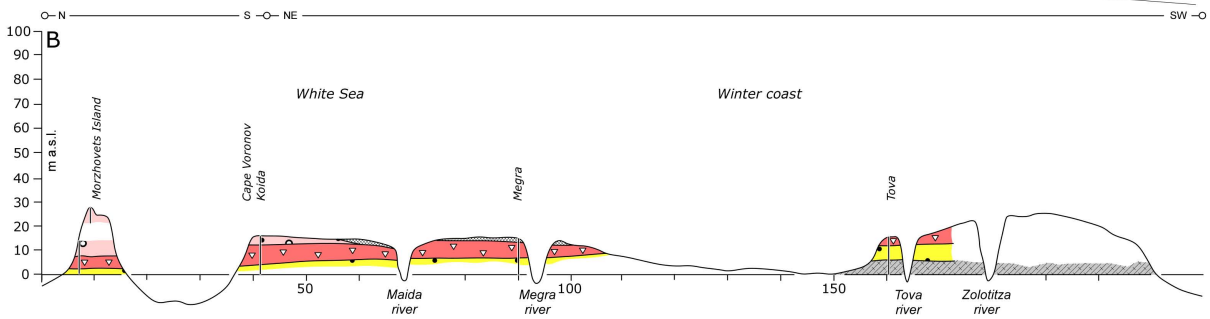
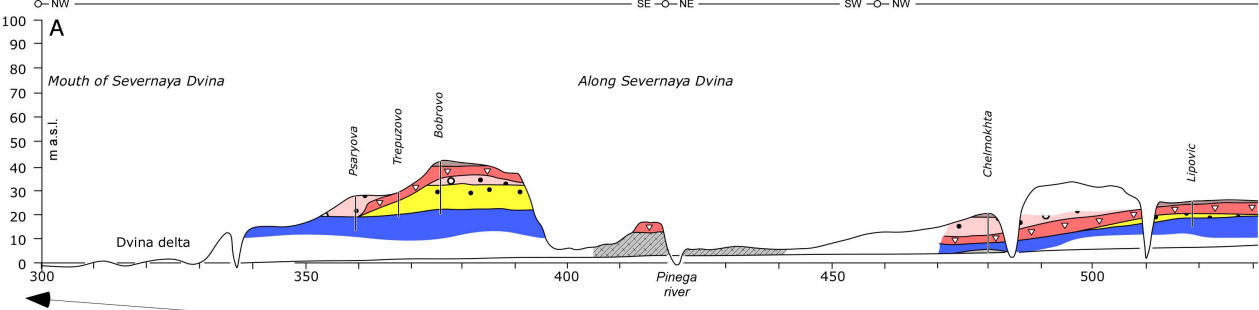
Tables

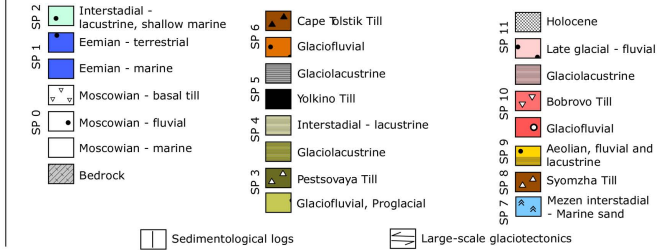
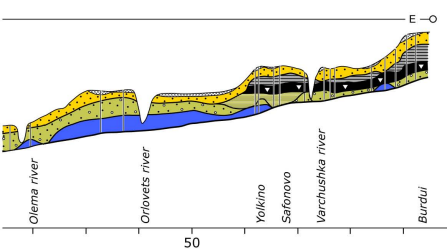
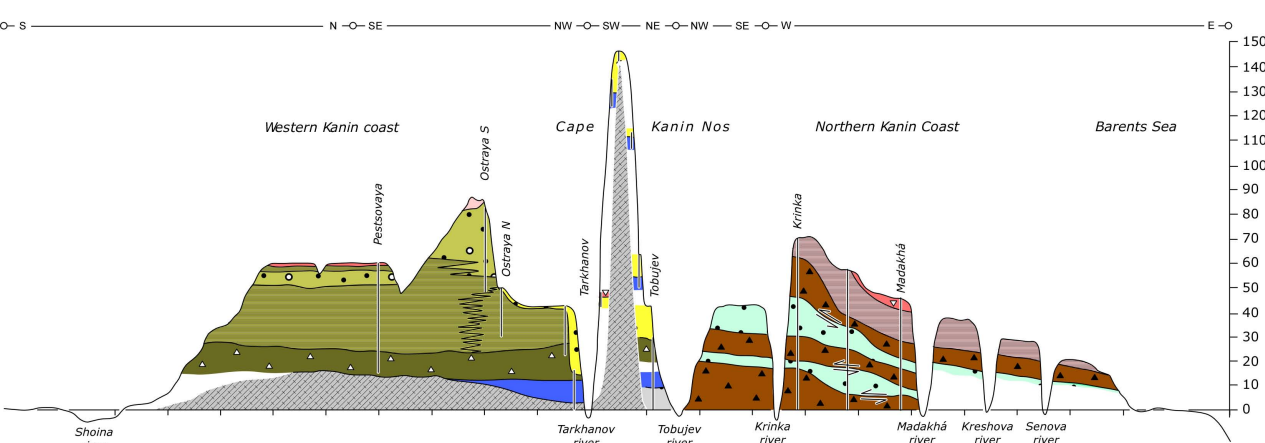
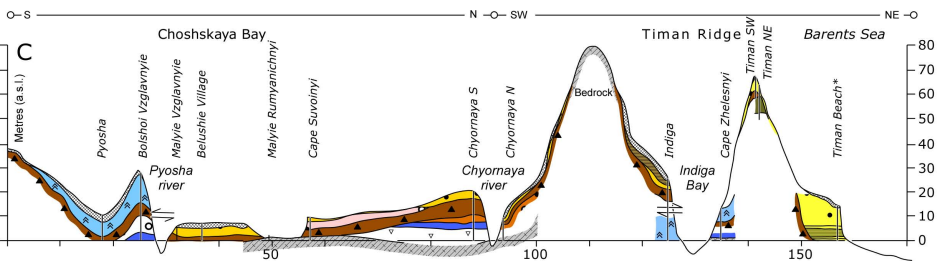
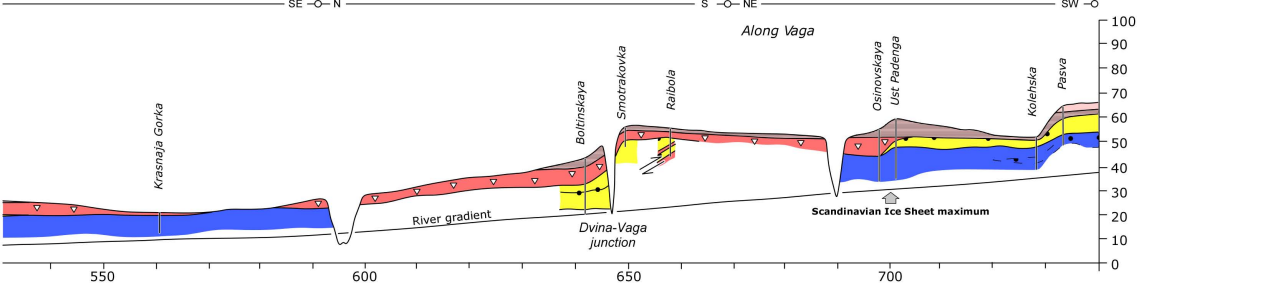
1. Optically stimulated luminescence dates from the Arkhangelsk region, NW Russia. More detailed descriptions and discussions are found in Larsen *et al.* (1999), Lyså *et al.* (2001), Houmark-Nielsen *et al.* (2001), Kjær *et al.* (2001, 2006), Demidov *et al.* (2006), and Thomas *et al.* (2006). Thomas *et al.* (2006), corrected for burial depth, whereas a constant burial depth of *c.* 4 m is used in this paper. Thus the age estimates are not directly comparable, but the corrected age (Thomas *et al.* 2006) is normally within the age range of one standard deviation of the uncorrected ages applied here.
2. Radiocarbon ages in years BP with one standard deviation. Calibrated ages are given with two standard deviations. Calibrations are according to Reimer *et al.* (2004).
3. Surface exposure age dating results from NW Russia based on *in situ* ^{10}Be concentration. See Linge *et al.* (2006b), for further details on sites, samples, AMS results, and calculation and interpretation of ages.

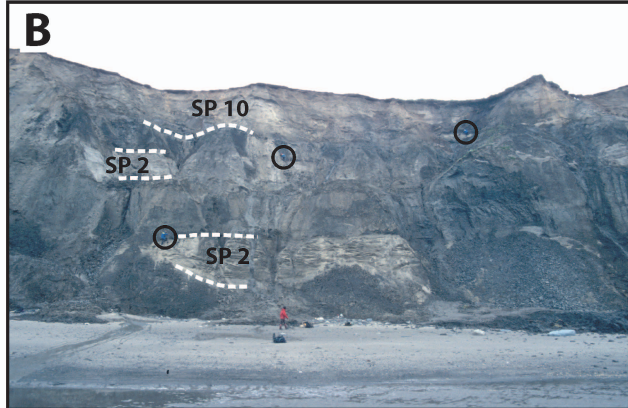


- 1: Koida
- 2: Cape Abramovsky
- 3: Cape Kargovsky
- 4: Cape Tolstik
- 5: Syomzha
- 6: Konushin
- 7: Pestsovaya
- 8: Tarkhanov
- 9: Madakha
- 10: Oiva
- 11: Bolshoi Vzglavnyie
- 12: Cape Zhelesnyie









A

Fluvial

SP 8. Syomzha Till

SP 7. Mezen
Interstadial

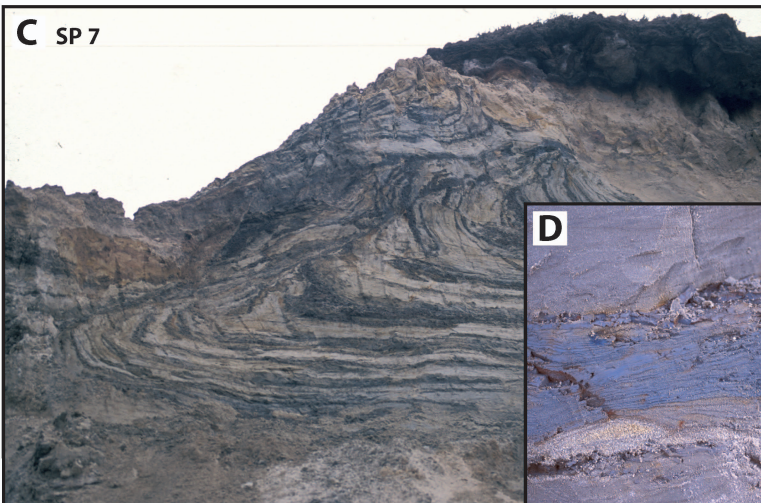
SP 6. Cape Tolstik Till

Fluvial / glaciofluvial

SP 5. Yolokino Till

B

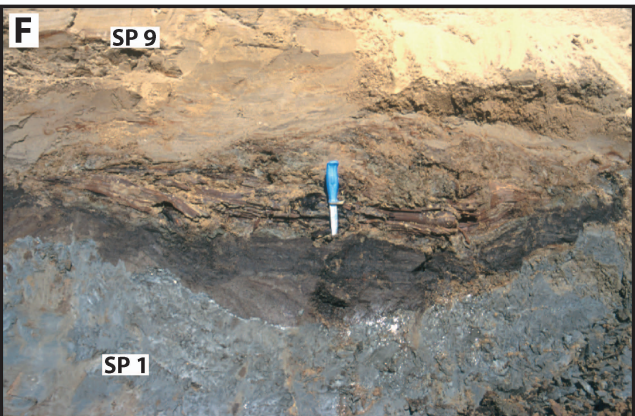
SP 5

**C** SP 7**D****E**

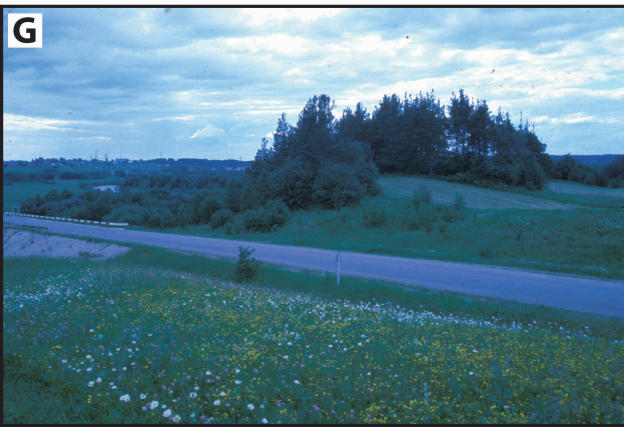
SP 8

**F**

SP 9

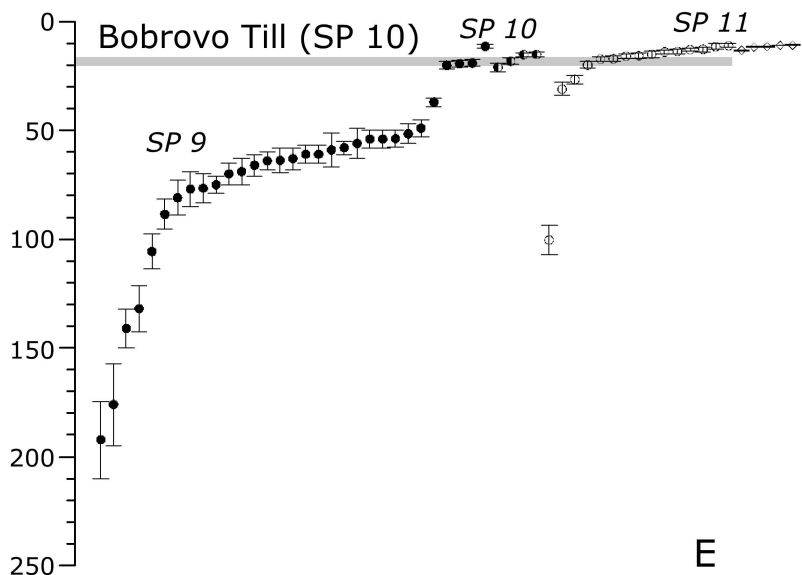
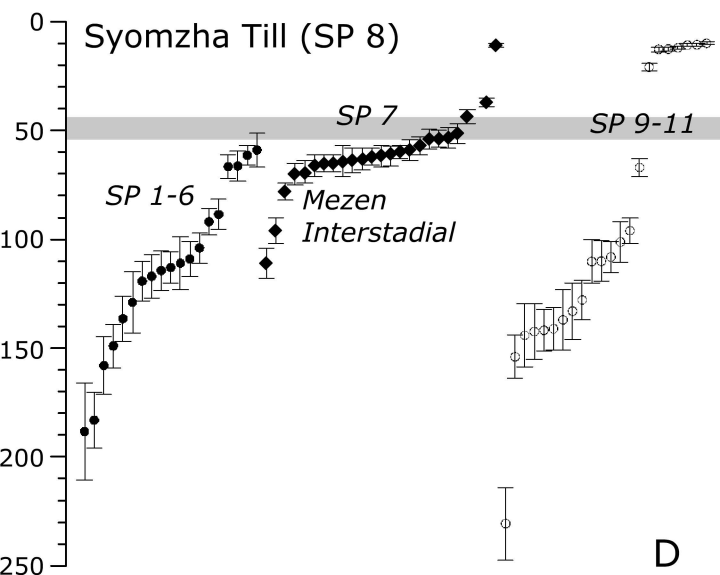
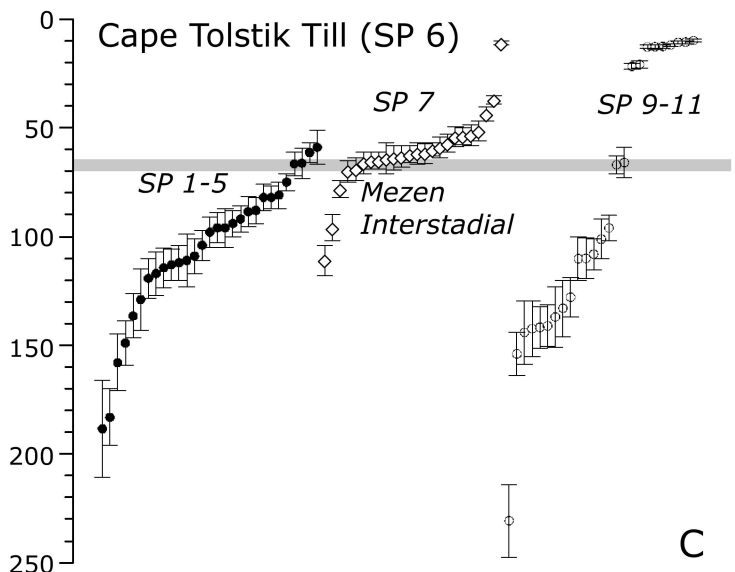
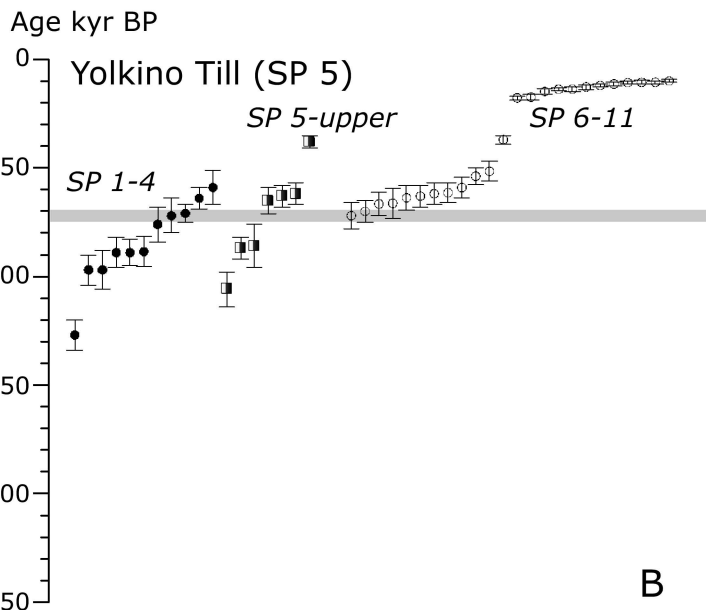
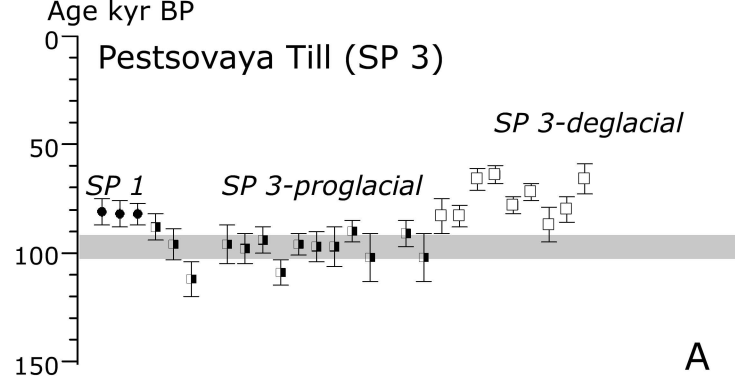
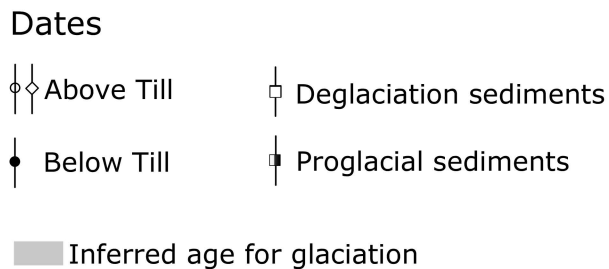


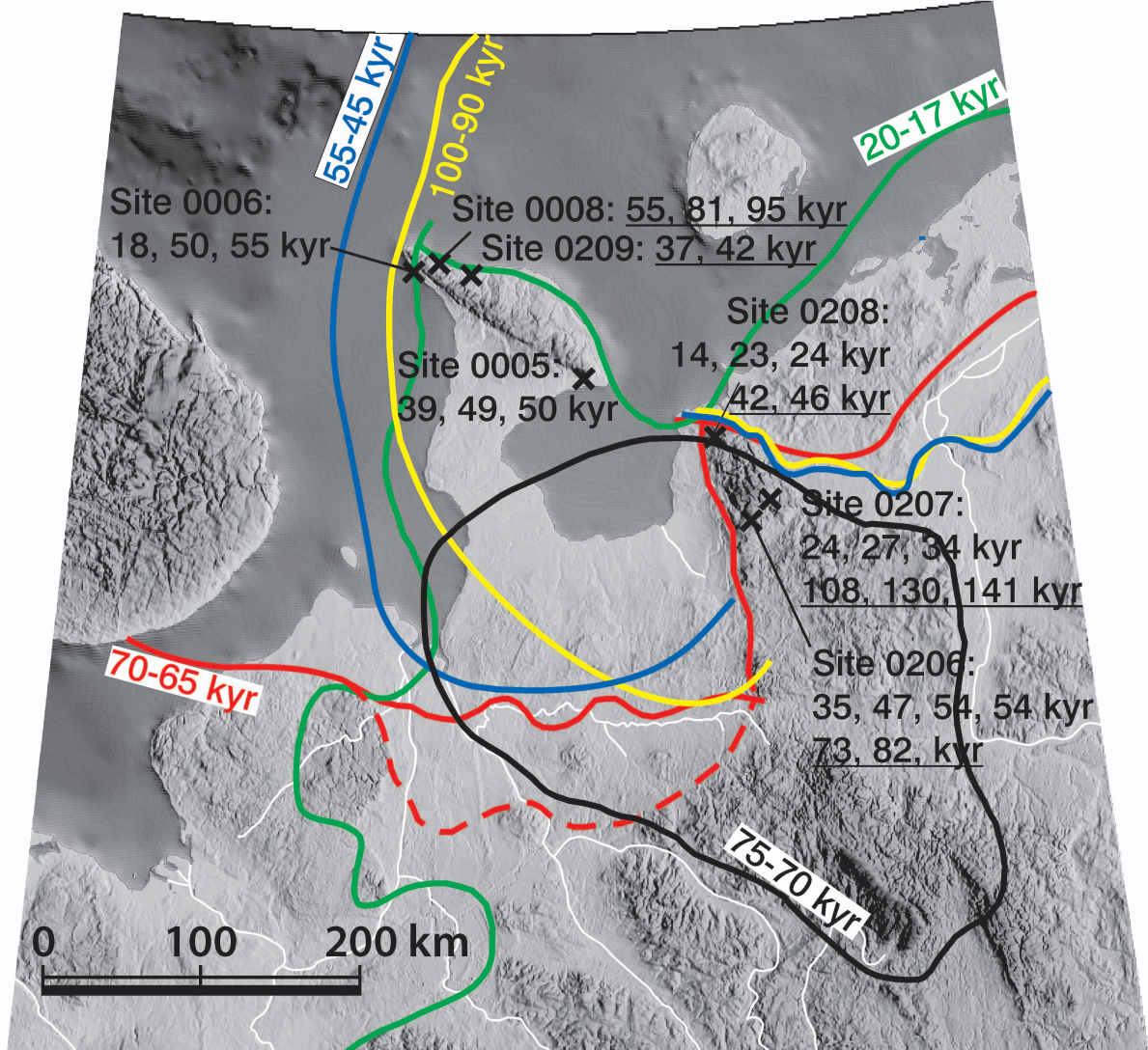
SP 1

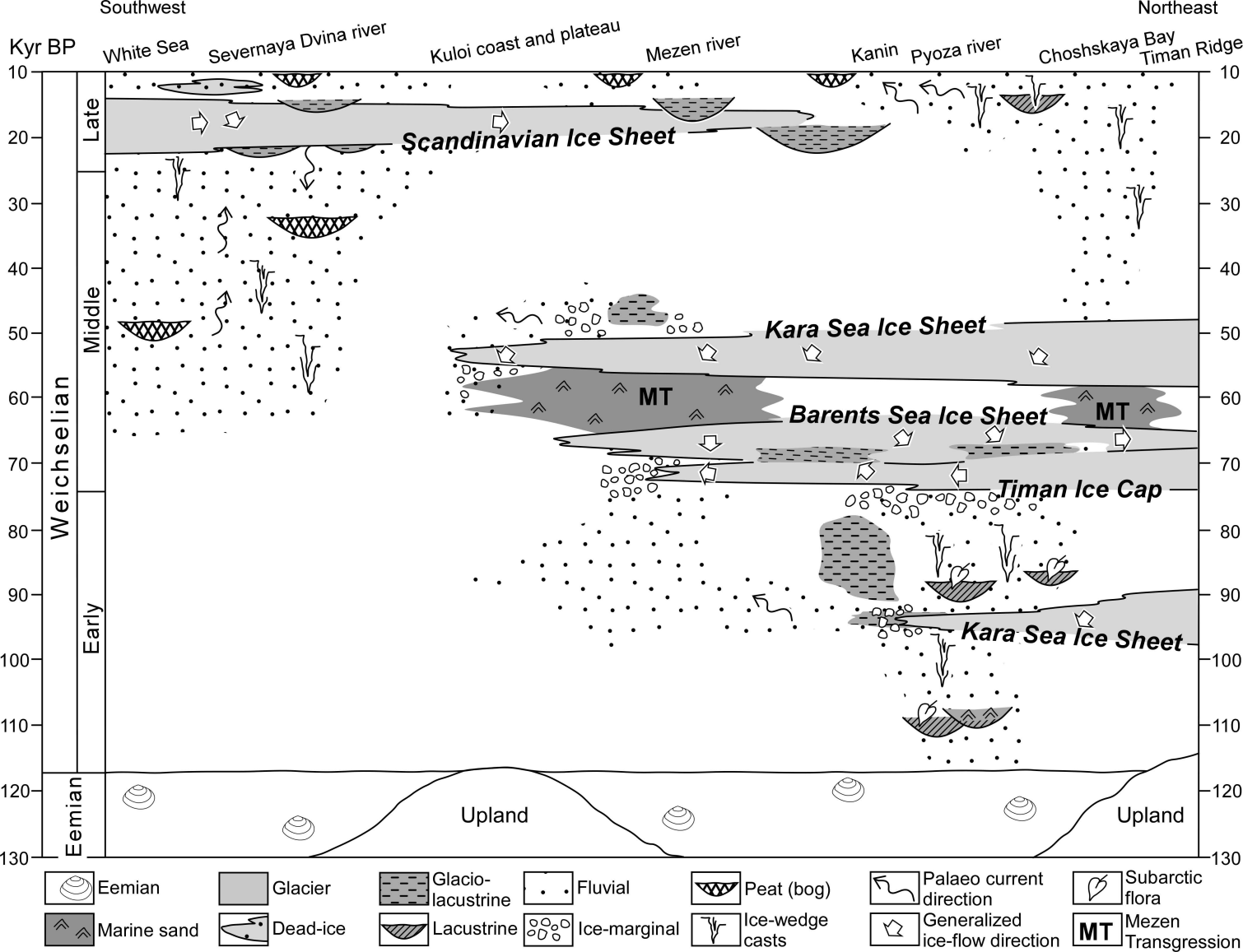
G**H**

SP 10









Legend



Glacier



Down-wasting ice



Sea



Lake



River plain



Drainage direction



Eolian field



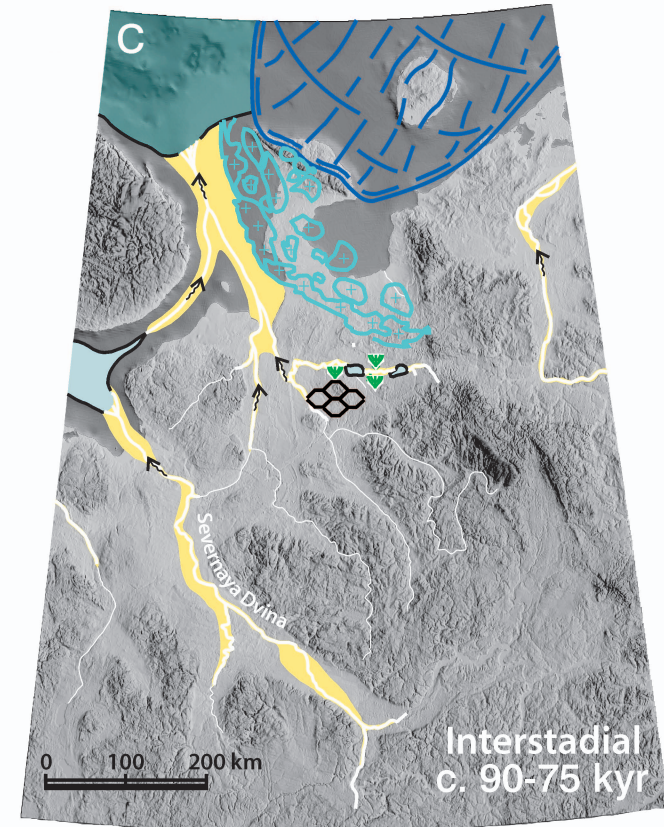
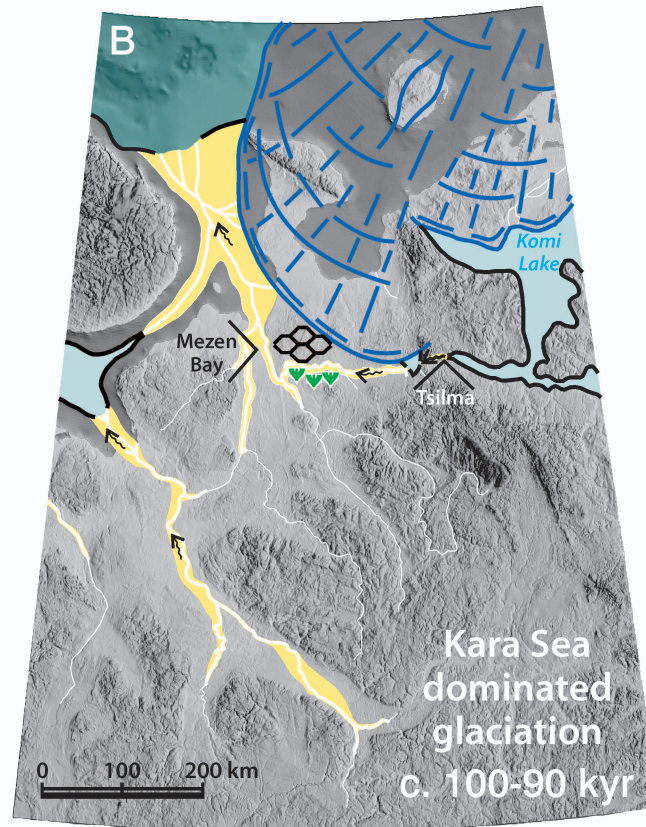
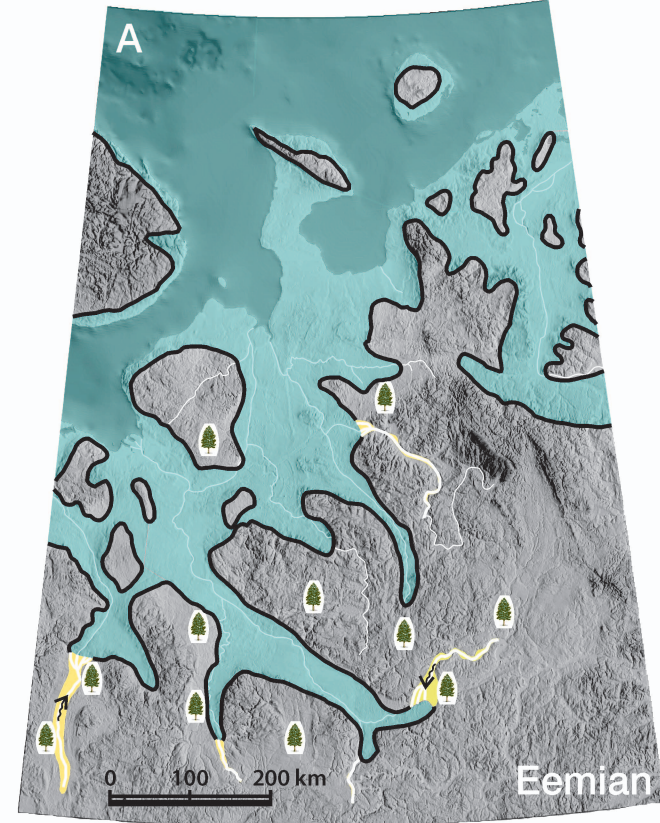
Permafrost (ice-wedge casts)

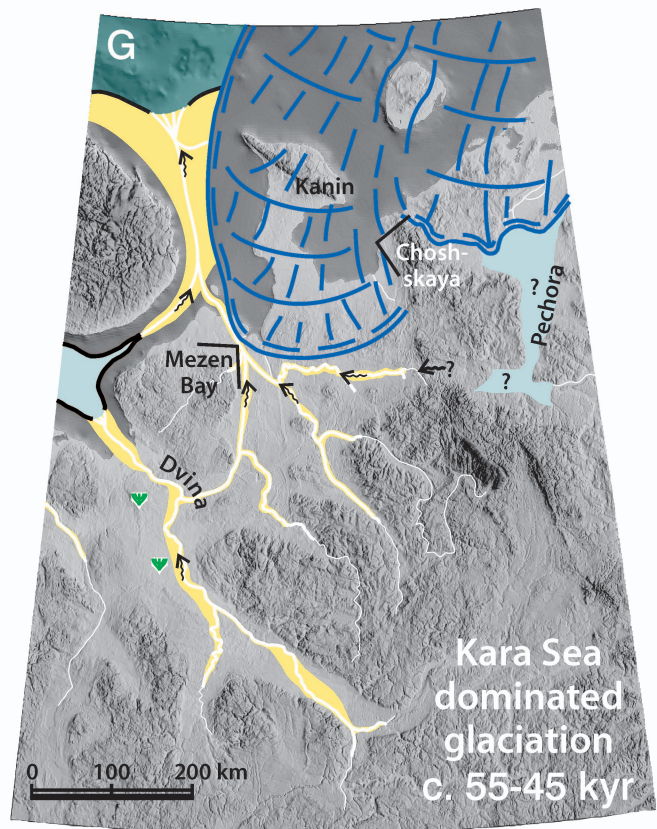
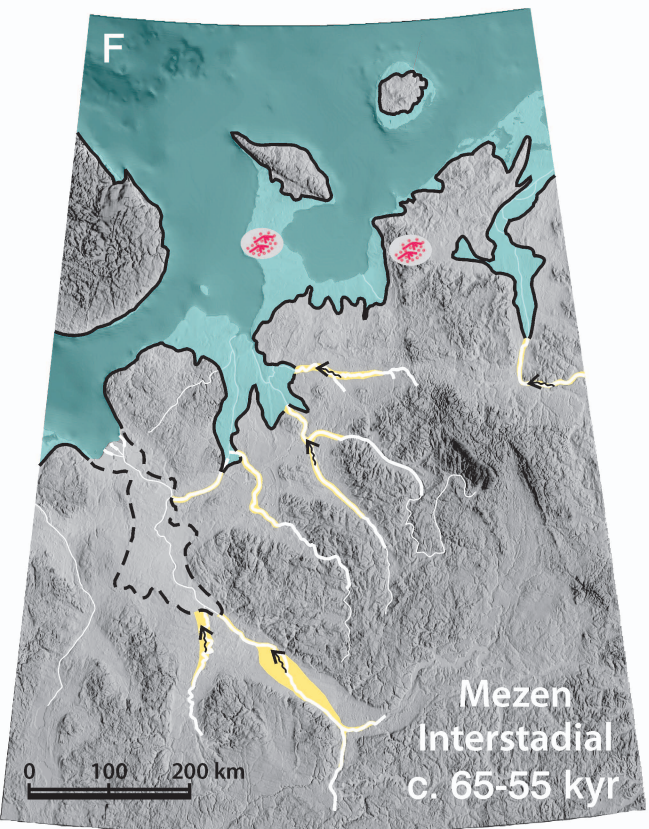
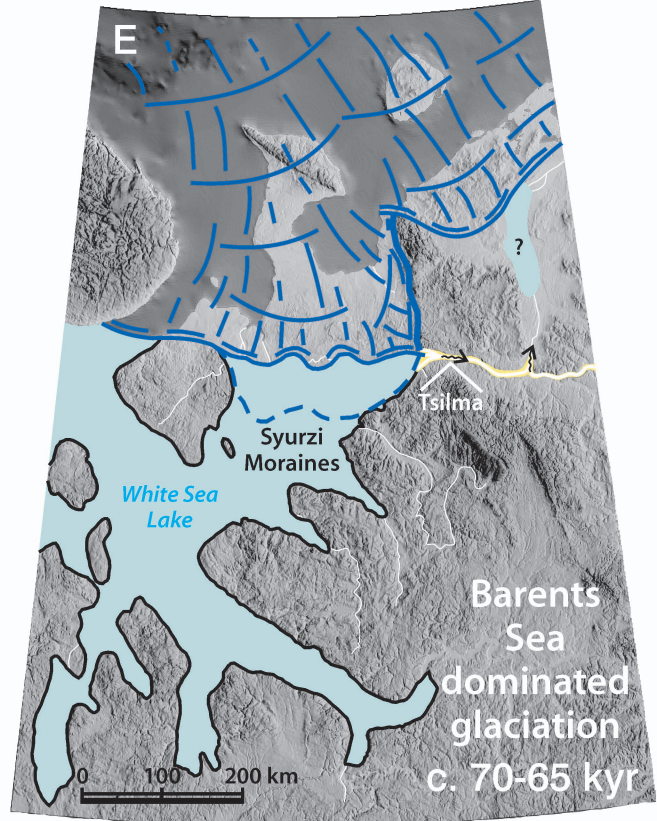
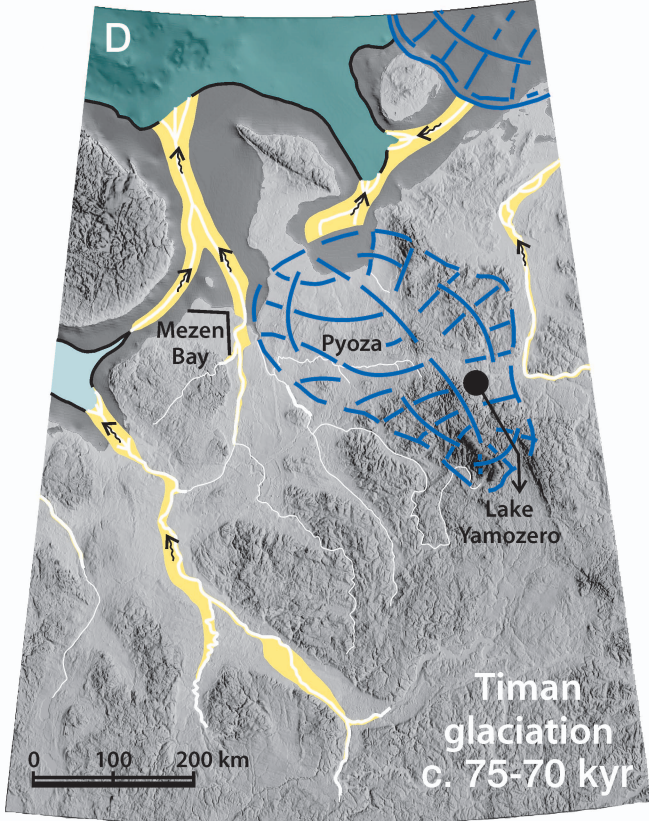


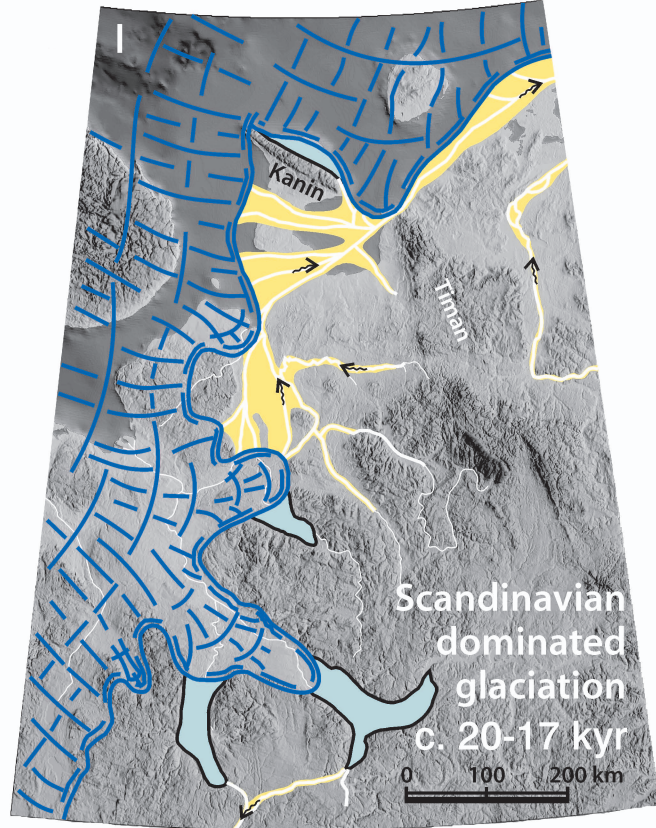
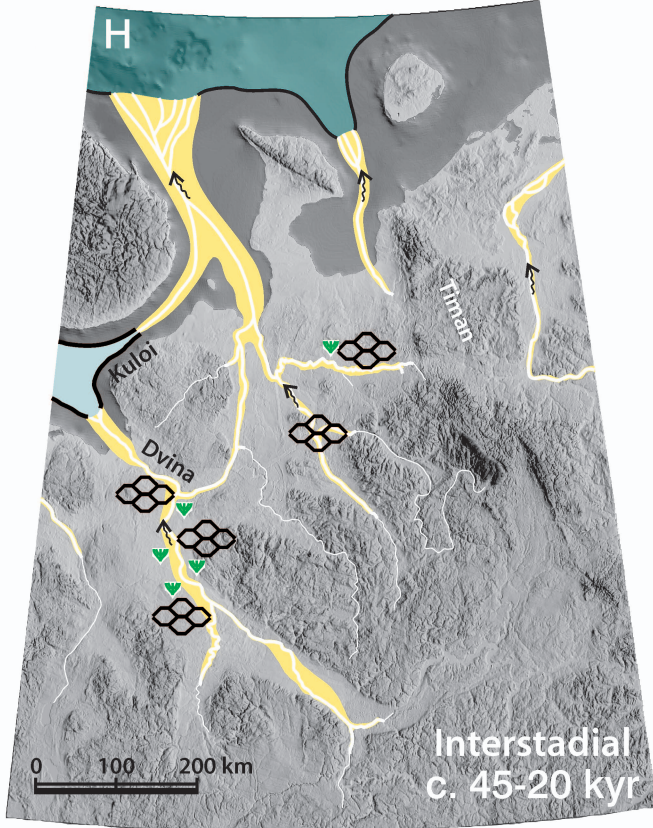
Tundra

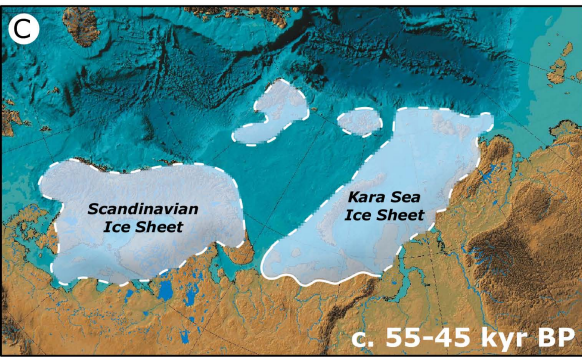
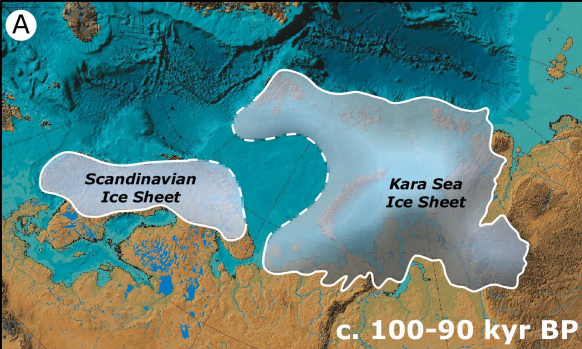


Taiga









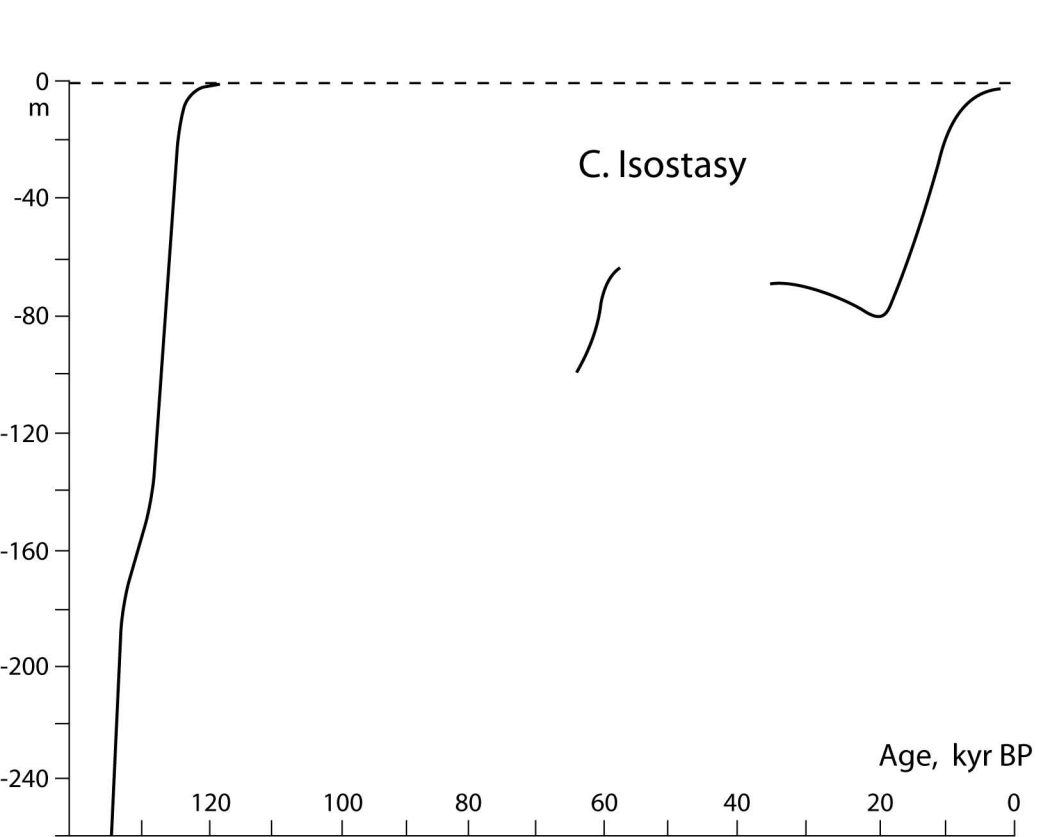
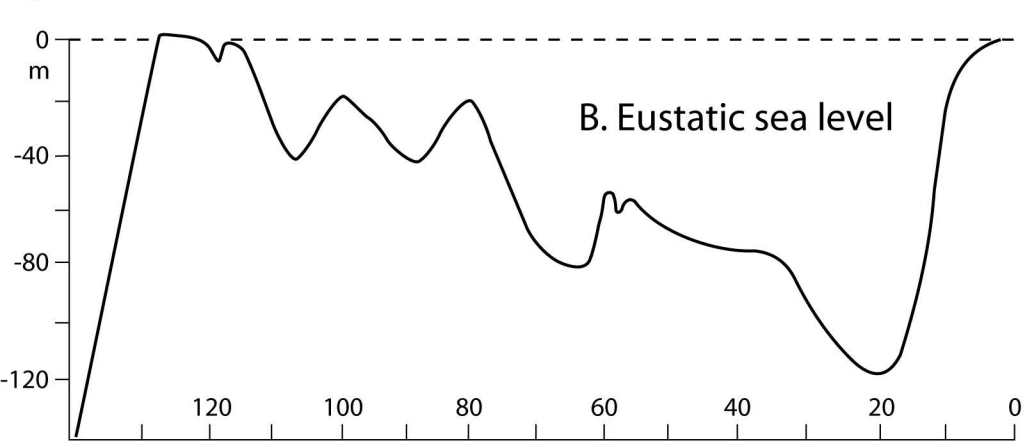
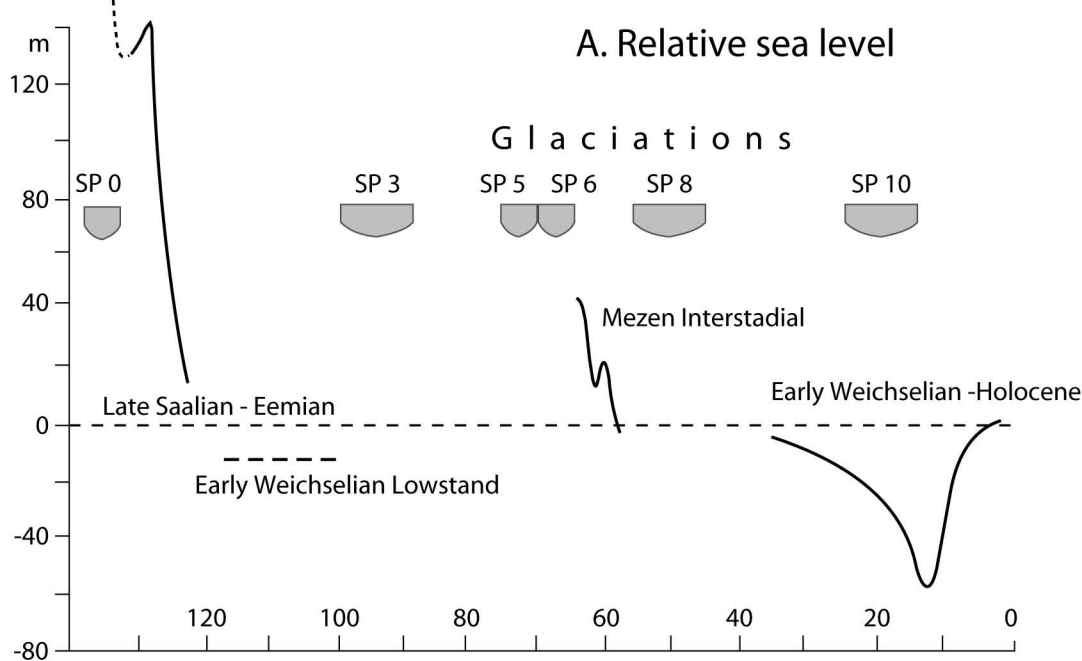


Table 1. Optically stimulated luminescence dates from the Arkhangelsk region, NW Russia. More detailed descriptions and discussions are found in Larsen *et al.* (1999), Lyså *et al.* (2001), Houmark-Nielsen *et al.* (2001), Kjær *et al.* (2001, 2006), Demidov *et al.* (2006), and Thomas *et al.* (2006). Thomas *et al.* (2006) corrected for burial depth, whereas a constant burial depth of *c.* 4 m is used in this paper. Thus the age estimates are not directly comparable, but the corrected age (Thomas *et al.* 2006) is normally within the age range of one standard deviation of the uncorrected ages applied here.

Lab. No.	Sample No.	Site name	Site No.	Lat. (N°)	Long. (E°)	m a.s.l.	Age, kyr	Dose (Gy)	(n)	Dose rate (Gy/ka)	w.c. %	Sediment	Stratigraphical position (Fig. 2)	References
001028	00-434	Shoina	0009	675321	440817	0,0	0,04 ± 0,013	0,038 ± 0	36	0,95 ± n/d	15	Tidal sand	Modern	
021014	02-517	Madakha	0209_50	683304	444411	0,0	1 ± 0	1,8 ± 0	24	1,68 ± 0,07	20	Beach	Modern	6)
021026	02-536	Krinka	0209_159	683304	444411	0,0	4 ± 1	4,1 ± 1	30	0,92 ± 0,05	22	Beach	Modern	6)
961002	96028	Pasva	9613	613539	424159	63,0	11,5 ± 1,3	24,1 ± n/d	n/d	2,09 ± n/d	n/d	Fluvial sand	11	1, 2)
961003	96038	Raibola	9615	620943	430059	47,0	17,2 ± 1,3	26,9 ± n/d	n/d	1,55 ± n/d	n/d	Fluvial sand	11	1, 2)
961005	96042	Raibola	9615	620943	430059	47,5	15,9 ± 1,2	17,8 ± n/d	n/d	1,12 ± n/d	n/d	Fluvial sand	11	1, 2)
963805	96043	Raibola	9615	620943	430059	55,5	17,1 ± 1,3	14,9 ± n/d	n/d	0,9 ± n/d	n/d	Fluvial sand	11	1, 2)
972501	96039	Raibola	9615	620943	430059	55,5	14 ± 0,9	21,4 ± n/d	n/d	1,53 ± n/d	n/d	Fluvial sand	11	1, 2)
972504	96029	Pasva	9613	613539	424159	63,0	12,9 ± 0,8	29,4 ± n/d	n/d	2,27 ± n/d	n/d	Fluvial sand	11	1, 2)
972508	97025	Chelmochta	9601	633903	413939	13,0	13,7 ± 1,1	32,9 ± n/d	n/d	2,39 ± n/d	n/d	Lacustrine sand	11	1, 2)
972509	97028	Chelmochta	9601	633903	413939	11,7	15,7 ± 1,2	36,2 ± n/d	n/d	2,29 ± n/d	n/d	Lacustrine sand	11	1, 2)
972516	97043	Pyoza	1	654801	450037	24,0	12,1 ± 1,2	30 ± 2	7	1,97 ± n/d	29	Fluvial sand	11	3)
983807	97044	Pyoza	1	654801	450037	23,0	11,9 ± 0,8	20,9 ± 1	12	1,75 ± n/d	30	Fluvial sand	11	3)
983815	98506	Varchushka	21	654602	475422	64,5	17,4 ± 1,2	13,4 ± 1	18	0,77 ± 0,03	30	Fluvial sand	11	3)
983816	98507	Varchushka	21	654602	475422	65,5	17,8 ± 0,9	31,6 ± 1	15	1,77 ± 0,04	30	Fluvial sand	11	3)
983822	98513	Pyoza	26	654103	481128	76,5	10,6 ± 0,8	6,3 ± 0	17	0,6 ± 0,02	30	Fluvial sand	11	3)
983826	98517	Pyoza	25	654049	480317	73,0	13,8 ± 0,7	13 ± 0	18	0,94 ± 0,03	30	Fluvial sand	11	3)
983827	98518	Pyoza	25	654049	480317	75,5	13,7 ± 1,1	20 ± 1	21	1,43 ± 0,05	30	Fluvial sand	11	3)
983829	98520	Pyoza	20	654304	474931	62,0	14,8 ± 1,2	16,5 ± 1	27	1,09 ± 0,03	30	Fluvial sand	11	3)
983830	98521	Pyoza	20	654304	474931	63,0	11,4 ± 0,7	9,4 ± 0	16	0,73 ± 0,03	30	Fluvial sand	11	3)
983840	98538	Pyoza	12	654133	465323	55,5	14,9 ± 0,9	20,2 ± 1	12	1,19 ± 0,04	30	Fluvial sand	11	3)
983843	98541	Pyoza	10	654218	462919	40,5	52 ± 5	29 ± 2	15	0,55 ± 0,02	30	Fluvial sand	11	3)
1038	99404	Svomzha	2_3	661049	440500	14,3	10,9 ± 0,8	20,7 ± 1	23	1,9 ± n/d	18	Tidal sand	11	4)
1039	99405	Svomzha	2_3	661049	440500	15,3	12,6 ± 1	21,7 ± 1	27	1,72 ± n/d	19	Fluvial sand	11	4)
1043	99429	Ezhuga	9910_2	641445	450007	21,2	26,6 ± 1,9	29,4 ± 1	21	1,11 ± n/d	18	Glaciolacustrine sand	11	
993817	99410	Kap Tolstik	1_5	660328	440440	17,9	10,6 ± 1	15,9 ± 0	18	1,5 ± n/d	18	Fluvial sand	11	4)
993818	99411	Kap Tolstik	1_5	660328	440440	18,3	10,8 ± 1	15,4 ± 0	18	1,43 ± n/d	15	Fluvial sand	11	4)
993819	99412	Kap Tolstik	1_4	660321	440432	14,3	9,9 ± 1	24,6 ± 1	18	2,48 ± n/d	19	Glaciolacustrine sand	11	4)
993820	99413	Kap Tolstik	1_4	660321	440432	15,3	12 ± 1	14,1 ± 0	18	1,17 ± n/d	22	Fluvial sand	11	4)
993828	99422	Kap Kargovsky	3_4	661106	434246	11,9	12,7 ± 1	23 ± 1	18	1,81 ± n/d	14	Fluvial sand	11	4)
993833	99427	Kologora	9906_3	644330	433116	4,5*	15 ± 2	18,2 ± 2	21	1,21 ± n/d	18	Aeolian sand	11	5)
993839	99433	Mezhdurechensky	9912_2	640246	442946	1,5*	100 ± 7	173,2 ± 3	18	1,72 ± n/d	12	Glaciolacustrine sand	11	5)
001031	00-437	Cape Abramovsky	0010_13	662403	431612	18,7	21 ± 1,7	24,9 ± 1	18	1,19 ± n/d	22	Fluvial sand	11	
001032	00-438	Koida	0011_06	662513	423758	3,8	31 ± 3	35,2 ± 2	21	1,15 ± n/d	27	Fluvial sand	11	
001034	00-440	Koida	0011_29	662513	423758	2,5	20 ± 1,4	25,3 ± 1	21	1,27 ± n/d	23	Fluvial sand	11	
001036	00-442	Morzhovets	0012_12	664531	422610	10,0	11 ± 0,9	15,4 ± 1	21	1,38 ± n/d	21	Glaciolacustrine sand	11	
961001	96026	Pasva	9613	613539	424159	60,0	21 ± 2	16,4 ± n/d	n/d	0,78 ± n/d	n/d	Fluvial sand	10	1, 2)
963806	96024	Koleshka	9612	613705	423931	50,7	15,2 ± 1	15,6 ± n/d	n/d	1,05 ± n/d	n/d	Lacustrine sand	10	1, 2)
963807	96030	Smotrakovka	9614	621311	430655	50,7	19,3 ± 1,6	19,4 ± n/d	n/d	1,04 ± n/d	n/d	Fluvial sand	10	1, 2)
963808	96031	Smotrakovka	9614	621311	430655	50,7	20,1 ± 1,6	18,9 ± n/d	n/d	0,88 ± n/d	n/d	Fluvial sand	10	1, 2)
972502	96025	Koleshka	9612	613705	423931	50,7	18,2 ± 1,5	17,4 ± n/d	n/d	0,94 ± n/d	n/d	Lacustrine sand	10	1, 2)
972503	96027	Pasva	9613	613539	424159	60,0	15,1 ± 1,1	13,4 ± n/d	n/d	0,88 ± n/d	n/d	Fluvial sand	10	1, 2)
001017	00-412	Oiva	0004_17	674860	461854	14,0	133 ± 13	272 ± 20	21	2,04 ± n/d	25	Lacustrine/fluviol	10	6)
001018	00-413	Oiva	0004_17	674860	461854	30,0	137 ± 14	266 ± 21	20	1,94 ± n/d	24	Lacustrine/fluviol	10	6)
001019	00-414	Oiva	0004_15	674860	461854	30,0	154 ± 10	242 ± 6	21	1,57 ± n/d	26	Lacustrine/fluviol	10	6)
001035	00-441	Morzhovets	0012_18	664531	422610	0,8	19 ± 1,5	15,8 ± 1	22	0,83 ± n/d	20	Glaciolacustrine sand	10	
011022	01520	Cape Suvoyni	0111_2	670960	474250	3,7	22 ± 1,2	22 ± 1	18	1,01 ± 0,05	36	Fluvial sand	10	6)
011025	01523	Indiga tundra	0114_B	674209	490526	64,6	67 ± 4	124 ± 6	33	1,86 ± 0,08	28	Lacustrine sand	10	6)
011029	01527	Indiga Guba	0115_B5	671240	484515	5,8	19 ± 1,3	27,5 ± 1	20	1,46 ± 0,07	34	Lacustrine sand	10	7)
021009	02-511	Madakha	0209_78	683304	444411	42,5	101 ± 9	158,1 ± 12	11	1,56 ± 0,06	27	Lacustrine sand	10	
021010	02-512	Madakha	0209_3	683304	444411	31,3	108 ± 7	208,6 ± 10	24	1,93 ± 0,08	27	Lacustrine sand	10	6)
021011	02-513	Madakha	0209_3	683304	444411	24,5	128 ± 9	190,7 ± 10	21	1,49 ± 0,06	31	Lacustrine sand	10	6)
021012	02-514	Madakha	0209_5	683304	444411	33,9	142 ± 9	152,7 ± 7	21	1,08 ± 0,05	28	Lacustrine sand	10	6)
021013	02-515	Madakha	0209_5	683304	444411	34,3	142 ± 13	156,9 ± 11	23	1,1 ± 0,05	21	Lacustrine sand	10	6)
021017	02-523	Madakha	0209_51	683304	444411	42,2	144 ± 14	181,3 ± 16	11	1,26 ± 0,05	27	Lacustrine sand	10	6)
021021	02-529	Krinka	0209_144	683304	444411	68,8	96 ± 6	161,1 ± 7	22	1,68 ± 0,06	31	Lacustrine sand	10	6)
021022	02-530	Krinka	0209_144	683304	444411	52,8	110 ± 10	172,8 ± 14	24	1,57 ± 0,06	29	Lacustrine sand	10	6)
021023	02-531	Krinka	0209_150	683304	444411	78,5	231 ± 17	219,2 ± 12	24	0,95 ± 0,04	29	Lacustrine sand	10	6)
021024	02-532	Krinka	0209_144	683304	444411	60,5	110 ± 9	119,9 ± 8	23	1,09 ± 0,05	23	Lacustrine sand	10	6)
021027	02-539	Krinka	0209_106	683304	444411		141 ± 10	210,7 ± 11	12	1,49 ± 0,06	28	Lacustrine sand	10	6)
961004	96040	Raibola	9615	620943	430059	51,0	54 ± 4	76,2 ± n/d	n/d	1,41 ± n/d	n/d	Fluvial sand	9	1, 2)
961006	96041	Raibola	9615	620943	430059	51,0	56 ± 7	85,7 ± n/d	n/d	1,52 ± n/d	n/d	Fluvial sand	9	1, 2)
972510	97004	Bobrovo	9701	642107	411019	31,2	66 ± 5	75,8 ± n/d	n/d	1,14 ± n/d	n/d	Fluvial sand	9	1, 2)
972511	97006	Bobrovo	9701	642107	411019	25,7	81 ± 8	65,9 ± n/d	n/d	0,82 ± n/d	n/d	Fluvial sand	9	1, 2)
972512	97008	Bobrovo	9701	642107	411019	23,8	49 ± 4	63,3 ± n/d	n/d	1,35 ± n/d	n/d	Fluvial sand	9	1, 2)
972515	97020	Trepuzovo	9603	642146	410253	21,2	54 ± 4	63,8 ± n/d	n/d	1,18 ± n/d	n/d	Fluvial sand	9	1, 2)
983801	97009	Bobrovo	9701	642107	411019	25,7	61 ± 4	81 ± n/d	n/d	1,33 ± n/d	n/d	Fluvial sand	9	1, 2)
983802	97021	Trepuzovo	9603	642146	410253	21,2	69 ± 6	85,1 ± n/d	n/d	1,22 ± n/d	n/d	Fluvial sand	9	1, 2)
983803	97007	Bobrovo	9701	642107	411019	23,8	61 ± 4	55 ± n/d	n/d	0,9 ± n/d	n/d	Fluvial sand	9	1, 2)
983804	97005	Bobrovo	9701	642107	411019	31,2	64 ± 4	64 ± n/d	n/d	1 ± n/d	n/d	Fluvial sand	9	1, 2)
011001	01403	E Tarkhanov	0116e	683223	434159	148,0	71 ± 4	97 ± 2	21	1,37 ± 0,07	27	Glaciolacustrine	9	6)
011030	01404	E Tarkhanov	0117	683223	434115	135,0	63 ± 5	96 ± 6	20	1,52 ± 0,07	32	Glaciolacustrine	9	6)
011003	01418	Maly Vzglavni	0108	665337	473244	5,0	13 ± 0,8	18,4 ± 1	21	1,44 ± 0,07	25	Fluvial sand	9	6)
021007	02-509	Timan	0208_4	673248	482624		75 ± 5	129,1 ± 5	24	1,73 ± 0,07	16	Aeolian	9	6)

1040	99417	Kargovsky	3_3	661148	434303	0,7	59 ± 8	88 ± 10	15	1,49 ± n/d	20	Glaciolacustrine sand	8	4)
1041	99424	Kargovsky	3_2	661134	434605	2,9	37 ± 2	76 ± 2	21	2,07 ± n/d	19	Tidal sand	7	4)
1042	99425	Kargovsky	3_1	661134	434605	3,6	70 ± 5	68 ± 2	19	0,97 ± n/d	20	Tidal sand	7	4)
993807	99400	Syomzha	2_2	660925	440557	9,3	62 ± 5	105 ± 4	15	1,7 ± n/d	24	Tidal sand	7	4)
993808	99401	Syomzha	2_2	660925	440557	6,0	44 ± 3	77,4 ± 3	21	1,77 ± n/d	20	Tidal sand	7	4)
993809	99402	Syomzha	2_2	660925	440557	5,3	54 ± 5	64,1 ± 4	25	1,19 ± n/d	23	Tidal sand	7	4)
993810	99403	Syomzha	2_2	660925	440557	3,8	53 ± 5	69,5 ± 4	24	1,3 ± n/d	20	Tidal sand	7	4)
993815	99408	Kap Tolstik	1_5	660328	440440	10,1	59 ± 5	56,4 ± 3	27	0,96 ± n/d	19	Tidal sand	7	4)
993816	99409	Kap Tolstik	1_5	660328	440440	11,5	62 ± 5	80,5 ± 4	27	1,3 ± n/d	21	Tidal sand	7	4)
993824	99418	Kap Kargovsky	3_1	661131	434720	1,5	63 ± 5	52,6 ± 3	21	0,83 ± n/d	17	Tidal sand	7	4)
993825	99419	Kap Kargovsky	3_1	661131	434720	2,2	64 ± 6	100,9 ± 6	21	1,58 ± n/d	21	Tidal sand	7	4)
993826	99420	Kap Kargovsky	3_4	661106	434246	2,5	54 ± 4	58,9 ± 3	21	1,1 ± n/d	21	Tidal sand	7	4)
993827	99421	Kap Kargovsky	3_4	661106	434246	4,0	52 ± 5	76,3 ± 5	21	1,48 ± n/d	21	Tidal sand	7	4)
001029	00-435	Cape Abramovsky	0010_18	662403	431612	1,4	57 ± 4	56 ± 2	21	0,98 ± n/d	20	Tidal sand	7	
001030	00-436	Cape Abramovsky	0010_17	662403	431612	2,8	64 ± 7	87 ± 8	25	1,36 ± n/d	23	Tidal sand	7	
011004	01420	Cape Zhelesnyi	0113_3	674309	484448	65,0	65 ± 4	99 ± 3	24	1,54 ± 0,07	13	Glaciolacustrine	7	6)
011005	01421	Cape Zhelesnyi	0113_3	674309	484448	65,0	32 ± 2	54 ± 3	27	1,67 ± 0,08	25	Fluvial sand?	7	6)
011018	01516	Cape Bolshoi Vzglavnyi	0105_12	665458	472721	3,7	78 ± 4	116 ± 2	21	1,48 ± 0,07	30	Tidal sand	7	6)
011019	01517	Cape Bolshoi Vzglavnyi	0105_12	665458	472721	6,4	60 ± 3	81 ± 2	26	1,34 ± 0,06	36	Tidal sand	7	6)
011020	01518	Cape Bolshoi Vzglavnyi	0105_9	665458	472721	16,0	69 ± 5	82 ± 3	15	1,19 ± 0,06	37	Tidal sand	7	6)
011021	01519	Cape Bolshoi Vzglavnyi	0105_7	665458	472721	8,0	62 ± 4	52 ± 1	21	0,84 ± 0,05	31	Tidal sand	7	6)
011023	01521	Cape Zhelesnyi	0112_54	674309	484448	13,1	65 ± 4	91 ± 3	21	1,39 ± 0,06	33	Marine sand	7	6)
011024	01522	Cape Zhelesnyi	0112_14	674309	484448	22,7	96 ± 6	176 ± 7	31	1,83 ± 0,07	29	Tidal sand	7	6)
011027	01525	Indiga Guba	0115_B0	671240	484515	5,4	66 ± 5	167 ± 8	27	2,52 ± 0,12	14	Lacustrine / Tidal sand	7	6)
011028	01526	Indiga Guba	0115_B1	671240	484515	16,8	111 ± 7	163 ± 6	20	1,48 ± 0,06	36	Tidal sand	7	6)
993814	99407	Kap Tolstik	1_5	660328	440440	6,0	61 ± 5	53,8 ± 2	15	0,88 ± n/d	16	Fluvial sand	6	4)
993821	99414	Kap Tolstik	1_6	660340	440436	5,7	67 ± 5	52,2 ± 3	15	0,78 ± n/d	16	Fluvial sand	6	4)
993822	99415	Kap Tolstik	1_6	660340	440436	5,9	66 ± 7	59,4 ± 5	21	0,9 ± n/d	19	Fluvial sand	6	4)
983811	98500	Varchushka	23	654826	475622	65,0	38 ± 3	96 ± 5	27	2,51 ± 0,06	30	Glaciolacustrine mud	5	3)
983817	98508	Varchushka	18	654310	474348	58,0	86 ± 10	181 ± 20	21	2,03 ± 0,05	30	Glaciolacustrine mud	5	3)
983818	98509	Varchushka	18	654310	474348	55,5	106 ± 8	143 ± 9	21	1,35 ± 0,03	30	Fluvial sand	5	3)
983820	98511	Pyoza	26	654103	481128	69,0	87 ± 5	209 ± 8	21	2,37 ± 0,06	30	Glaciolacustrine mud	5	3)
983821	98512	Pyoza	26	654103	481128	70,0	63 ± 5	206 ± 12	27	3,23 ± 0,1	30	Glaciolacustrine mud	5	3)
983824	98515	Pyoza	25	654049	480317	60,5	72 ± 6	55 ± 3	21	0,78 ± 0,03	30	Fluvial sand	5	3)
983828	98519	Pyoza	25	654049	480317	68,0	62 ± 5	174 ± 12	27	2,74 ± 0,08	30	Glaciolacustrine mud	5	3)
983831	98522	Pyoza	17	654126	474341	60,0	65 ± 6	143 ± 11	14	2,24 ± 0,07	30	Glaciolacustrine mud	5	3)
983832	98523	Pyoza	17	654126	474341	55,5	72 ± 8	128 ± 14	25	1,74 ± 0,05	30	Fluvial sand	5	3)
983833	98527	Pyoza	15	654214	473352	55,0	71 ± 4	69 ± 3	15	0,96 ± 0,03	30	Fluvial sand	5	3)
983835	98529	Pyoza	13	654106	473047	56,0	64 ± 5	71 ± 4	15	1,08 ± 0,03	30	Glaciolacustrine mud	5	3)
983834	98528	Pyoza	15	654214	473352	52,5	76 ± 8	64 ± 6	15	0,81 ± 0,03	30	Fluvial sand	4	3)
983836	98530	Pyoza	13	654106	473047	53,0	89 ± 6	71 ± 3	21	0,69 ± 0,02	30	Fluvial sand	4	3)
983837	98531	Pyoza	13	654106	473047	51,5	89 ± 7	111 ± 6	15	1,22 ± 0,04	30	Glaciolacustrine mud	4	3)
972517	97046	Pyoza	1	654801	450037	22,0	102 ± 11	85 ± 7	4	0,84 ± n/d	29	Fluvial sand	3	3)
972518	97048	Pyoza	4	655020	455744	36,0	150 ± 18	194 ± 20	4	1,3 ± n/d	29	Fluvial sand	3	3)
983806	97047	Pyoza	1	654801	450037	22,0	91 ± 6	100 ± 4	24	1,11 ± n/d	30	Fluvial sand	3	3)
983813	98504	Varchushka	22	654651	475651	62,5	96 ± 5	98 ± 3	27	1,01 ± 0,03	30	Glaciolacustrine mud	3	3)
983814	98505	Varchushka	22	654651	475651	61,5	109 ± 6	111 ± 4	18	1,96 ± 0,04	30	Glaciolacustrine mud	3	3)
983819	98510	Pyoza	26	654103	481128	63,5	97 ± 7	188 ± 9	21	1,94 ± 0,05	30	Glaciolacustrine mud	3	3)
983825	98516	Pyoza	24	654043	480003	60,5	97 ± 9	78 ± 6	21	0,68 ± 0,02	30	Fluvial sand	3	3)
983839	98537	Pyoza	12	654133	465323	53,5	90 ± 5	85 ± 3	15	0,93 ± 0,02	30	Fluvial sand	3	3)
1044	99430	Ezhuga	9910_2	641445	450007	16,0	75 ± 4	125 ± 1	18	1,66 ± n/d	16	Fluvial sand	3	
993829	99423	Kap Kargovsky	3_5	660933	433653	16,5	89 ± 7	100,2 ± 5	33	1,13 ± n/d	20	Glaciolacustrine sand	3	4)
993832	99426	Kologora	9906_1	644330	433116	2,05*	77 ± 7	107,5 ± 6	21	1,4 ± n/d	18	Glaciolacustrine sand	3	5)
993837	99431	Mezhdurechensky	9912_1	640244	442904	2,1*	141 ± 9	112,3 ± 0	18	0,8 ± n/d	22	Glaciolacustrine sand	3	5)
993838	99432	Mezhdurechensky	9912_1	640244	442904	3,8*	106 ± 8	104 ± 5	21	0,98 ± n/d	22	Glaciolacustrine sand	3	5)
001005	00-400	Konushinskaya Korga	0001_21	671011	435034	7,4	98 ± 7	110 ± 5	18	1,11 ± n/d	23	Fluvial sand	3	6)
001006	00-401	Konushinskaya Korga	0001_21	671011	435034	7,7	96 ± 9	100 ± 8	45	1,05 ± n/d	23	Fluvial sand	3	6)
001007	00-402	Konushinskaya Korga	0001_18	671011	435034	7,0	75 ± 4	93,4 ± 1	39	1,25 ± n/d	24	Marine sand	3	6)
001008	00-403	Konushinskaya Korga	0001_18	671011	435034	10,8	112 ± 8	128 ± 5	21	1,15 ± n/d	18	Aeolian sand?	3	6)
001009	00-404	Konushinskaya Korga	0001_11	671011	435034	16,0	96 ± 7	106 ± 4	18	1,1 ± n/d	22	Aeolian sand	3	6)
001010	00-405	Konushinskaya Korga	0001_80	671011	435034	28,0	88 ± 6	182 ± 8	23	2,06 ± n/d	25	Lacustrine sand?	3	6)
001011	00-406	Konushinskaya Korga	0002_	671037	434934	34,0	66 ± 7	148 ± 12	18	2,26 ± n/d	11	Lacustrine sand?	3	6)
001012	00-407	Konushinskaya Korga	0001_11	671011	435034	4,6	82 ± 5	115 ± 3	21	1,4 ± n/d	21	Fluvial sand?	3	6)
001013	00-408	Cape Konushin	0003_09	671148	434635	10,0	82 ± 6	106 ± 5	21	1,29 ± n/d	22	Marine mud	3	6)
001014	00-409	Cape Konushin	0003_15	671148	434635	19,0	81 ± 6	106 ± 4	21	1,31 ± n/d	25	Marine sand	3	6)
001015	00-410	Cape Konushin	0003_15	671148	434635	21,0	94 ± 6	121 ± 3	21	1,29 ± n/d	24	Aeolian sand	3	6)
001020	00-421	Tarkhanov	0006_0	683052	433557	32,1	80 ± 6	142 ± 5	21	1,78 ± n/d	23	Glaciolacustrine	3	6)
001021	00-423	Tarkhanov	0006_0	683052	433557	29,4	87 ± 8	165 ± 11	20	1,89 ± n/d	25	Glaciolacustrine	3	6)
001025	00-431	Tobojev	0008_2	683323	434838	36,0	77 ± 6	86 ± 4	20	1,11 ± n/d	32	Marine sand	3	6)
001033	00-439	Koida	0011_06	662513	423758	9,5	11 ± 0,7	20,6 ± 0	21	1,81 ± n/d	17	Lacustrine sand	3	
001037	00-444	Tova	0014_0	654743	402630	9,1	77 ± 8	70 ± 6	27	0,91 ± n/d	28	Marine sand?	3	
011002	01405	S of Tarkhanov river	0118	682939	433958	45,0	58 ± 3	94 ± 3	24	1,62 ± 0,07	31	Fluvial sand?	3	6)
011006	01500	Pestsovaya	0101_5	681939	440838	28,5	72 ± 4	118 ± 3	18	1,66 ± 0,07	33	Fluvial sand	3	6)
011007	01501	Pestsovaya	0101_5	681939	440838	30,2	78 ± 4	115 ± 3	21	1,47 ± 0,07	41	Fluvial sand	3	6)
011008	01502	Pestsovaya	0101_5	681939	440838	53,2	64 ± 4	99 ± 4	27	1,56 ± 0,07	37	Lacustrine sand	3	6)
011009	01503	Pestsovaya	0101_3	681939	440838	51,4	66 ± 5	87 ± 6	24	1,31 ± 0,06	28	Shoreface sand	3	6)
011010	01504	Pestsovaya	0101_3	681939	440838	53,0	83 ± 5	101 ± 3	18	1,21 ± 0,06	29	Shoreface sand	3	6)
011011	01505	Pestsovaya	0101_3	681939	440838	51,0	83 ± 8	109 ± 3	21	1,33 ± 0,11	29	Shoreface sand	3	6)
011012	01506	Ostraya	0102_6	682456	435451	35,0	80 ± 4	128 ± 1	18	1,6 ± 0,07	37	Glaciolacustrine	3	6)
011013	01507	Ostraya	0102_6	682456	435451	49,3	82 ± 6	121 ± 7	30	1,47 ± 0,06	36	Glaciolacustrine	3	6)
011014	01508	Ostraya	0102_8	682456	435451	54,5	50 ± 4	121 ± 7	27	2,44 ± 0,1	30	Lacustrine sand	3	6)
001022	00-427	River Krinker	0007_7	683219	441727	43,3	158 ± 13	247 ± 13	18	1,56 ± n/d	24	Lacustrine sand	2	6)

001023	00-428	River Krinker	0007_7	683219	441727	36,0	117 ± 10	235 ± 15	21	2 ± n/d	18	Lacustrine sand	2	6)
001024	00-429	River Krinker	0007_3	683219	441727	6,5	129 ± 14	270 ± 25	20	2,09 ± n/d	14	Marine sand	2	6)
001026	00-432	River Krinker	0007_25	643419	435112	28,0	111 ± 12	220 ± 20	20	1,99 ± n/d	27	Marine sand	2	6)
001027	00-433	River Krinker	0007_25	643419	435112	37,0	149 ± 10	284 ± 8	26	1,91 ± n/d	27	Marine sand	2	6)
021015	02-518	Madakha	0209_53	683304	444411	5,9	114 ± 9	165,5 ± 11	11	1,45 ± 0,06	28	Shoreface sand	2	6)
021016	02-520	Madakha	0209_53	683304	444411	11,4	183 ± 13	126,9 ± 5	11	0,69 ± 0,04	26	Shoreface sand	2	6)
021018	02-524	Madakha	0209_53	683304	444411	12,8	188 ± 22	157,3 ± 17	10	0,84 ± 0,04	25	Shoreface sand	2	6)
021019	02-526	Madakha	0209_55	683304	444411	19,5	137 ± 10	190,4 ± 11	24	1,4 ± 0,06	26	Lacustrine sand	2	6)
021020	02-527	Madakha	0209_55	683304	444411	20,0	119 ± 9	160,8 ± 10	21	1,35 ± 0,05	32	Lacustrine sand	2	6)
021025	02-535	Krinka	0209_158	683304	444411	23,8	92 ± 6	150,1 ± 7	35	1,63 ± 0,06	32	Tidal sand	2	6)
021028	02-540	Krinka	0210_15	644355	500847	11,5	631 ± 113	165,5 ± 21	8	0,26 ± 0,03	30	Tidal sand	2	6)
021029	02-541	Krinka	0210_15	644355	500847	19,5	116 ± 10	170,3 ± 11	12	1,47 ± 0,08	32	Lacustrine sand	2	6)
983838	98533	Pyoza	14	654106	473047	50,5	127 ± 7	165 ± 4	24	1,38 ± 0,04	30	Marine sand	1	3)
011015	01509	Chyomaya	0103_0	672715	475631	7,7	104 ± 7	100 ± 4	21	0,97 ± 0,05	29	Marine sand (tidal)	1	6)
011016	01510	Chyomaya	0103_0	672715	475631	7,0	109 ± 8	105 ± 4	24	0,96 ± 0,06	29	Marine sand (tidal)	1	6)
021001	02-500	Tsibjuga	0203_0	650747	464022	19,0	115 ± 9	77,7 ± 4	12	0,68 ± 0,04	26	Sand	1	7)
021002	02-501	Tsibjuga	0203_0	650747	464022	19,2	124 ± 12	71,3 ± 5	12	0,57 ± 0,04	24	Sand	1	7)
972519	97052	Pyoza	5	654928	455850	14,5	127 ± 8	175 ± 4	4	1,38 ± n/d	29	Glaciofluvial sand	0	3)
983805	97053	Pyoza	5	654928	455850	42,5	190 ± 20	214 ± 22	17	1,14 ± n/d	30	Glaciofluvial sand	0	3)
983808	97049	Pyoza	4	655020	455744	36,5	102 ± 11	156 ± 14	23	1,52 ± n/d	30	Fluvial sand	0	3)
983841	98539	Pyoza	10	654218	462919	31,5	260 ± 30	298 ± 26	24	1,06 ± 0,04	30	Fluvial sand	0	3)
983842	98540	Pyoza	10	654218	462919	34,5	220 ± 20	289 ± 21	15	1,3 ± 0,03	30	Fluvial sand	0	3)
983844	98543	Pyoza	5	654928	455850	40,5	228 ± 12	250 ± 7	15	1,08 ± 0,03	30	Glaciofluvial sand	0	3)
983845	98544	Pyoza	5	654928	455850	41,0	217 ± 13	339 ± 10	15	1,11 ± 0,04	30	Glaciofluvial sand	0	3)
983846	98545	Pyoza	5	654928	455850	29,0	237 ± 12	247 ± 5	21	1,04 ± 0,03	30	Marine sand	0	3)
983847	98546	Pyoza	4	655020	455744	28,5	194 ± 13	225 ± 5	15	1,16 ± 0,06	30	Marine sand	0	3)
983848	98547	Pyoza	4	655020	455744	27,5	202 ± 14	220 ± 7	15	1,08 ± 0,05	30	Marine sand	0	3)
983849	98548	Ust Kyma	9824	644910	472712	44,0	260 ± 30	293 ± 23	33	1,03 ± 0,05	30	Fluvial sand	0	
983851	98550	Ust Kyma	9825	644941	472027	71,3	250 ± 20	235 ± 17	14	0,92 ± 0,05	30	Glaciofluvial sand	0	
983852	98551	Ust Kyma	9825	644941	472027	73,7	171 ± 14	393 ± 26	33	2,17 ± 0,06	30	Glaciofluvial sand	0	
993840	99434	Mezhdurechensky	9913	640322	441028	1,1*	132 ± 11	138,9 ± 7	19	1,05 ± n/d	18	Glaciofluvial sand	0	5)
993843	99437	Verkola	9915	634938	451150	9,1*	176 ± 19	150,5 ± 13	27	0,85 ± n/d	21	Glaciofluvial sand	0	5)
993844	99438	Verkola	9915	634938	451150	9,55*	192 ± 18	291,9 ± 20	21	1,52 ± n/d	21	Glaciofluvial sand	0	5)
001016	00-411	Oiva	0004_17	674860	461854	6,5	113 ± 7	259 ± 7	21	2,28 ± n/d	21	Lacustrine/fluvial	0	6)
011017	01511	Chyomaya	0103_17	672715	475631	8,5	183 ± 13	135 ± 5	27	0,74 ± 0,04	29	Glaciofluvial sand	0	6)
011026	01524	Indiga tundra	0114_D	674615	490514	11,2	127 ± 7	206 ± 6	21	1,62 ± 0,07	30	Fluvial sand	0	6)
021003	02-502	Sula	0204_4	644902	482251	21,0	237 ± 16	187,3 ± 8	22	0,79 ± 0,04	22	Lacustrine sand	0	
021004	02-504	Sula	0204_4	644902	482251	20,0	320 ± 24	173,2 ± 6	28	0,54 ± 0,03	26	Lacustrine sand	0	
021005	02-505	Sula	0204_4	644902	482251	2,5	311 ± 25	179,8 ± 9	24	0,58 ± 0,03	28	Lacustrine sand	0	
021006	02-508	Sula	0204_6	644902	482251	3,0	269 ± 23	162,4 ± 7	23	0,6 ± 0,04	29	Lacustrine sand	0	
021008	02-510	Timan	0208_2	673248	482624		531 ± 57	197,5 ± 10	21	0,37 ± 0,03	30	Bedrock sand		

References: 1) Larsen *et al.* (1999). 2) Lyså *et al.* (2001). 3) Houmark-Nielsen *et al.* (2001). 4) Kjær *et al.* (2003). 5) Demidov *et al.* (2006). 6) Kjær *et al.* (2006). 7) Thomas *et al.* (2006).

Table 2: Radiocarbon ages in years BP with one standard deviation. Calibrated ages are given with two standard deviations. Calibrations are according to Reimer *et al.* (2004).

Lab. Ref.	Sample code	Site	Dated material	Dry weight	¹⁴ C age yr BP	Calibrated age yr BP	Stratigraphic position (Fig. 2)
T-13321	97002	Psaryovo	Indifferent	7.4 g	11 355 ± 70	13 360-13 100	11
T-13172	97018	Trepuzovo	<i>Picea</i>	5.0 g	42 600 +1550/-1300		9
T-13173	97024	Chelmochta	<i>Salix/Populus</i>	5.0 g	9930 ± 135	12 000-11 100	11
T-13174	97030	Chelmochta	<i>Larix/Picea</i>	4.5 g	9635 ± 75	11 200-10 740	11
T-13175	97035	Chelmochta	<i>Salix/Populus</i>	1.7 g	9775 ± 115	11 650-10 750	11
T-13176	97042(1)	Chelmochta	<i>Salix/Populus</i>	1.3 g	9630 ± 125	11 250-10 550	11
T-13177	97042(2)	Chelmochta	<i>Betula</i>	6.5 g	9750 ± 135	11 650-10 700	11
AAR-3451	96112	Raibola	Indifferent		>50 000		9
		Raibola			24 900 ± 490 ¹⁾		9
AAR-7937	0106.085	Belushie	<i>Pinus?</i>		11 910 ± 90	14 000-13 550	11
UA-15158	98801	Ust Varchuska	<i>Dryas octopetala</i>	10.0g	12 610 ± 235	15 550-13 950	11
TUA-2946	97045	Bychye	Moss/Plant detrit		11 040 ± 75	13 100-12 860	11
TUA-1881	97045	Bychye	<i>Salix</i>		12 325 ± 100	14 850-13 950	11
TUA-1882	97045	Bychye	<i>Salix</i>		12 225 ± 80	14 500-13 800	11

¹⁾ Atlasov *et al.* (1978).

Table 3. Surface exposure age dating results from NW Russia based on *in situ* ^{10}Be concentration. See Linge *et al.* (2006b), for further details on sites, samples, AMS results, and calculation and interpretation of ages.

Sample ID	Site	Altitude (m a.s.l.)	Sample description	^{10}Be surface exposure age $\pm 1\sigma$ (kyr)
00-418	0006	115	Quartz vein in mica schist	51.71 \pm 3.24
00-419		100	Quartz vein in mica schist	55.20 \pm 3.97
00-420		50	Quartz vein/inclusion in meta-sandstone	18.14 \pm 1.57
00424	0008	130	Plagioclase granite, erratic boulder	94.91 \pm 7.47
00-425		125	Granite, erratic boulder	54.87 \pm 6.17
00-426		113	Granite, erratic boulder	80.93 \pm 5.63
02-521	0209	60	Granite, erratic boulder	36.51 \pm 2.98
02-522		60	Granite, erratic boulder	41.82 \pm 3.02
00-415	0005	74	Quartz vein in mica schist	39.38 \pm 3.38
00-416		138	Quartz vein in mica schist	48.65 \pm 3.83
00-417		150	Quartz inclusion in mica schist	50.42 \pm 4.09
02-411	0208	135	Sandstone, bedrock	22.78 \pm 1.64
02-412		135	Sandstone, bedrock	24.25 \pm 2.12
02-413		138	Granite, erratic boulder	42.36 \pm 3.25
02-414		137	Sandstone, bedrock	14.26 \pm 1.26
02-415		137	Gneiss, erratic boulder	45.98 \pm 3.26
02-406	0207	176	Sandstone, bedrock	26.98 \pm 2.13
02-407		179	Sandstone, bedrock	23.69 \pm 1.74
02-408		171	Sandstone, bedrock	34.37 \pm 3.83
02-409		148	Granite, erratic boulder	107.9 \pm 7.3
02-410a		148	Granite, erratic boulder	140.9 \pm 9.2
02-410b		148	Granite, erratic boulder	130.1 \pm 8.5
02-400	0206	245	Sandstone, bedrock	53.80 \pm 3.92
02-401		246	Sandstone, bedrock	35.38 \pm 2.43
02-402		235	Granite, erratic boulder	72.57 \pm 4.85
02-403		240	Sandstone, bedrock	53.79 \pm 3.49
02-404		240	Sandstone, bedrock	47.04 \pm 3.19
02-405		235	Granite, erratic boulder	81.85 \pm 5.79